

Modular grad-div stabilization for multiphysics flow problems

Mine Akbas^{*} Leo G. Rebholz[†]

Abstract

This paper considers a modular grad-div stabilization method for approximating solutions of two multiphysics flow problems: incompressible non-isothermal flows governed by the Boussinesq equations, and magnetohydrodynamics (MHD). The proposed methods add a minimally intrusive step to an existing Boussinesq/MHD code, with the key idea being that the penalization of the divergence errors, is only in the extra step (i.e. nothing is added to the original equations). The paper provides a full mathematical analysis by proving unconditional stability and optimal convergence of the methods considered. Numerical experiments confirm theoretical findings, and show that the algorithms have a similar positive effect as the usual grad-div stabilization.

1 Introduction

Classical conforming finite element discretizations for incompressible flows relax the divergence constraint, and enforce it only weakly. While this enables one to construct inf-sup stable discretizations, weak enforcement leads to errors depending on the continuous pressure scaled by the Reynolds number, and creates inaccurate computed solutions for many flow problems, including Boussinesq flows [18, 40, 11, 17, 14, 15], potential and generalized Beltrami flows [31, 30, 25], quasi-geostrophic flows [44, 7, 31], and two-phase flows with surface tension [16, 29].

One commonly used technique to overcome this issue in conforming mixed finite element methods is to use grad-div stabilization, which has been recently studied from both theoretical and computational points of view [36, 38, 32, 23, 5]. The studies show that it improves the accuracy of the approximate solutions for the Stokes/Navier-Stokes and related coupled multiphysics problems by reducing the effect of the continuous pressure on the velocity error [11, 45, 37, 36, 28, 38, 24, 35, 15]. However there are also disadvantages: this stabilization increases coupling in the linear system, and leads to linear algebraic systems often more difficult to solve since the matrix contribution to the velocity block is singular.

Recently, a variant of grad-div stabilization was introduced **for the incompressible NSE in [12]**, which is more attractive from an implementation standpoint. The proposed algorithm in [12] adds a minimally intrusive module which is used after each time step in a Navier-Stokes solver. This extra step implements **the first order** grad-div stabilization separately, and penalizes the divergence of the velocity error, both in L^2 and L^∞ -norms. Hence, the algorithm retains benefits of classical grad-div stabilization, but adds resistance to solver breakdown as the stabilization parameters increase. **The application of the grad-div step for any multistep time discretization can be found in [42] where the numerical scheme which uses second order grad-div step was analyzed and performed for the NSE.**

The purpose of this paper is to extend these novel ideas from [12] **to incompressible non-isothermal fluid flows governed by the Boussinesq equations, and from [42] to the magnetohydrodynamic (MHD) equations.** The numerical scheme for the Boussinesq equations consists of two steps. The first step approximates the usual Boussinesq equations with the backward Euler temporal and finite element spatial discretizations. The second step is a post processing step, and introduces a decoupled, **first order** grad-div stabilization step for the velocity. The proposed numerical method for MHD equations, on the other hand, **introduces two**

^{*}Department of Mathematics, Duzce University, 81620, Duzce, Turkey; mineakbas@duzce.edu.tr.

[†]Department of Mathematical Sciences, Clemson University, Clemson, SC 29634; rebholz@clemson.edu; This work was partially supported by NSF grant DMS1522191.

modular, second order grad-div steps, one each for the velocity and the magnetic field, into a MHD solver based on BDF2LE time and finite element spatial discretization. We make a note here that the first order grad-div step was applied to MHD equations in [34] where the evolution equations of the MHD model can be given in a different way. The novelty of these algorithms is that grad-div steps are decoupled from evolution equations, and hence they can be easily used with an existing code. Moreover, since the grad-div steps are separate, the penalization can happen without the negative effects on the saddle point system which can occur when parameters are bigger than one. This paper studies the stability and convergence properties of the proposed methods, and provides numerical experiments to illustrate their reliability and effectiveness. This paper is arranged as follows. Section 2 gathers necessary notation and mathematical preliminaries. Section 3 introduces a modular grad-div stabilization method for the incompressible Boussinesq equations, and studies its stability and convergence. It also presents some numerical experiments to test the effectiveness and reliability of the method. We proceed similarly in Section 4 for the MHD. In both cases, we compare results to usual grad-div stabilization. The last section summarizes the results of the paper.

2 Mathematical Preliminaries

This section introduces mathematical preliminaries and notation. We assume that Ω in \mathbb{R}^d ($d = 2, 3$) is a polygonal or polyhedral domain with the boundary $\partial\Omega$. Standard notation of Lebesgue and Sobolev spaces are used throughout this paper. The inner product in $(L^2(\Omega))^d$, is denoted by (\cdot, \cdot) , the norm in $(L^2(\Omega))^d$ by $\|\cdot\|$ and the norm in the Hilbert space $(H^k(\Omega))^d$ by $\|\cdot\|_k$. For X being a normed function space in Ω , $L^p(0, T; X)$ is the space of all functions defined on $(0, T) \times \Omega$ for which the norm is bounded

$$\|u\|_{L^p(0, T; X)} := \int_0^T \|u\|_X^p d\mathbf{x}, \quad p \in [1, \infty).$$

For $p = \infty$, the usual modification is used in the definition of this space. We consider the classical function spaces

$$\begin{aligned} \mathbf{X} : &= (H_0^1(\Omega))^d := \{\mathbf{v} \in (L^2(\Omega))^d : \nabla \mathbf{v} \in L^2(\Omega)^{d \times d}, \mathbf{v} = \mathbf{0} \text{ on } \partial\Omega\}, \\ Q : &= L_0^2(\Omega) := \{q \in L^2(\Omega) : \int_{\Omega} q \, dx = 0\}, \\ W : &= H_0^1(\Omega). \end{aligned}$$

For \mathbf{f} an element in the dual space of \mathbf{X} , its norm is defined by

$$\|\mathbf{f}\|_{-1} := \sup_{\mathbf{v} \in \mathbf{X}} \frac{(\mathbf{f}, \mathbf{v})}{\|\mathbf{v}\|_{L^2}}.$$

In this setting, we have the Poincaré-Friedrichs' inequality: $\forall v \in W$

$$\|v\|_{L^2} \leq C_P \|\nabla v\|_{L^2},$$

where C_P is a constant depending only on the size of Ω [27]. We define the trilinear forms:

$$\begin{aligned} b(\mathbf{u}, \mathbf{v}, \mathbf{w}) &:= \frac{1}{2} ((\mathbf{u} \cdot \nabla \mathbf{v}, \mathbf{w}) - (\mathbf{u} \cdot \nabla \mathbf{w}, \mathbf{v})), \quad \forall \mathbf{u}, \mathbf{v}, \mathbf{w} \in \mathbf{X}, \\ b^*(\mathbf{u}, \varphi, \psi) &:= \frac{1}{2} ((\mathbf{u} \cdot \nabla \varphi, \psi) - (\mathbf{u} \cdot \nabla \psi, \varphi)), \quad \forall \mathbf{u} \in \mathbf{X}, \text{ and } \forall \varphi, \psi \in W. \end{aligned}$$

The discrete time analysis needs the following norms: for $-1 \leq k < \infty$

$$\|v^n\|_{\infty, k} := \max_{1 \leq n \leq N} \|v^n\|_k, \quad \|v^n\|_{p, k} := \left(\Delta t \sum_{n=0}^{N-1} \|v^n\|_k^p \right)^{1/p}.$$

The following lemma is necessary to bound the trilinear terms in the analysis.

Lemma 2.1. *There exists a constant C such that for all $\mathbf{u}, \mathbf{v}, \mathbf{w} \in \mathbf{X}$*

$$\begin{aligned} b(\mathbf{u}, \mathbf{v}, \mathbf{w}) &= (\mathbf{u} \cdot \nabla \mathbf{v}, \mathbf{w}) + \frac{1}{2} ((\nabla \cdot \mathbf{u}) \mathbf{v}, \mathbf{w}), \\ b(\mathbf{u}, \mathbf{v}, \mathbf{w}) &\leq C \|\nabla \mathbf{u}\|_{L^2} \|\nabla \mathbf{v}\|_{L^2} \|\nabla \mathbf{w}\|_{L^2}, \\ b(\mathbf{u}, \mathbf{v}, \mathbf{w}) &\leq C \sqrt{\|\mathbf{u}\|_{L^2} \|\nabla \mathbf{u}\|_{L^2}} \|\nabla \mathbf{v}\|_{L^2} \|\nabla \mathbf{w}\|_{L^2}. \end{aligned}$$

Proof. Application of Hölder's inequality, interpolation theorem, the Sobolev embedding theorem and Poincaré inequality yield the result, see [27]. \square

For a spatial discretization, we consider a conforming finite element spaces $\mathbf{X}_h \subset \mathbf{X}, Q_h \subset Q, Y_h \subset W$ defined on a regular triangulation \mathcal{T}_h of the domain Ω with maximum diameter h . For the stability of the pressure, (\mathbf{X}_h, Q_h) is assumed to satisfy the discrete inf-sup condition: there is a constant α independent of the mesh size h such that

$$\inf_{q_h \in Q_h} \sup_{\mathbf{v}_h \in \mathbf{X}_h} \frac{(q_h, \nabla \cdot \mathbf{v}_h)}{\|\nabla \mathbf{v}_h\|_{L^2} \|q_h\|_{L^2}} \geq \alpha > 0. \quad (2.1)$$

We also assume that the finite element spaces (\mathbf{X}_h, Q_h, Y_h) , satisfy approximation properties of piecewise polynomials of local degree $k, k-1$, and k , respectively,

$$\inf_{\mathbf{v}_h \in \mathbf{X}_h} \{ \|\mathbf{u} - \mathbf{v}_h\|_{L^2} + h \|\nabla(\mathbf{u} - \mathbf{v}_h)\|_{L^2} \} \leq Ch^{k+1} \|\mathbf{u}\|_{k+1}, \quad (2.2)$$

$$\inf_{q_h \in Q_h} \|p - q_h\|_{L^2} \leq Ch^k \|p\|_k, \quad (2.3)$$

$$\inf_{\theta_h \in Y_h} \{ \|\theta - \theta_h\|_{L^2} + h \|\nabla(\theta - \theta_h)\|_{L^2} \} \leq Ch^{k+1} \|\theta\|_{k+1}. \quad (2.4)$$

The discretely divergence-free subspace of \mathbf{X}_h is defined by:

$$\mathbf{V}_h := \{ \mathbf{v}_h \in \mathbf{X}_h : (q_h, \nabla \cdot \mathbf{v}_h) = 0, \forall q_h \in Q_h \}.$$

It is known that under the inf-sup condition (2.1), the discretely divergence-free subspace \mathbf{V}_h has the same approximation properties as \mathbf{X}_h [6]:

$$\inf_{\mathbf{v}_h \in \mathbf{V}_h} \|\nabla(\mathbf{u} - \mathbf{v}_h)\|_{L^2} \leq C(\alpha) \inf_{\mathbf{v}_h \in \mathbf{X}_h} \|\nabla(\mathbf{u} - \mathbf{v}_h)\|_{L^2}.$$

Our finite element analysis needs the standard inverse inequality: for any $\mathbf{v} \in \mathbf{X}_h$,

$$\|\nabla \mathbf{v}\|_{L^2} \leq C_{inv} h^{-1} \|\mathbf{v}\|_{L^2},$$

where C_{inv} depends on the minimum angle in the triangulation. In our convergence analysis, we need a different version of the usual discrete Gronwall's Lemma in literature, see e.g., [21]:

Lemma 2.2 (Discrete Gronwall's Lemma). *Let $\Delta t, B$ and a_n, b_n, c_n, d_n be finite non-negative numbers such that*

$$a_N + \Delta t \sum_{n=0}^N b_n \leq \Delta t \sum_{n=0}^{N-1} d_n a_n + \Delta t \sum_{n=0}^N c_n + B \quad \text{for } N \geq 1.$$

Then for all $\Delta t > 0$,

$$a_N + \Delta t \sum_{n=0}^N b_n \leq \exp\left(\Delta t \sum_{n=0}^{N-1} d_n\right) \left(\Delta t \sum_{n=0}^N c_n + B\right) \quad \text{for } N \geq 1.$$

3 First order modular grad-div stabilization for the Boussinesq equations

This section presents a modular grad-div method based on backward-Euler time and finite element spatial discretizations for the incompressible Boussinesq equations, and gives its stability and convergence results. In addition, numerical experiments show the efficiency of the proposed method.

Incompressible, non-isothermal fluid flows are governed by the incompressible Navier-Stokes equations (NSE) and heat transport equation, and read as: for a given force field $\mathbf{f} : (0, T] \times \Omega \rightarrow \mathbb{R}^d$, find a velocity field $\mathbf{u} : (0, T] \times \Omega \rightarrow \mathbb{R}^d$, and pressure and temperature fields $p, \theta : (0, T] \times \Omega \rightarrow \mathbb{R}$ such that (\mathbf{u}, p, θ) satisfies the equations

$$\begin{aligned} \frac{\partial \mathbf{u}}{\partial t} - \nu \Delta \mathbf{u} + \mathbf{u} \cdot \nabla \mathbf{u} + \nabla p &= Ri \langle \mathbf{0}, \theta \rangle + \mathbf{f}, \quad \text{in } (0, T] \times \Omega, \\ \nabla \cdot \mathbf{u} &= 0, \quad \text{in } (0, T] \times \Omega, \\ \frac{\partial \theta}{\partial t} - \kappa \Delta \theta + (\mathbf{u} \cdot \nabla) \theta &= \Psi, \quad \text{in } (0, T] \times \Omega, \end{aligned} \quad (3.1)$$

with appropriate boundary and initial conditions. The problem is posed on a bounded domain with Lipschitz continuous boundary. Here, $\nu := Re^{-1}$ is the dimensionless kinematic viscosity, where Re denotes the Reynolds number, $Ri := Gr/Re^2$ is the Richardson number which accounts for the gravitational force and the thermal expansion of the fluid, and $\kappa := 1/(PrRe)$ is thermal diffusivity coefficient. The modular grad-div stabilization method is given as follows:

Algorithm 3.1. Let body forces \mathbf{f}, Ψ , initial velocity \mathbf{u}_0 and temperature θ_0 , and the stabilization parameters $\gamma \geq 0, \beta \geq 0$ be given. Set \mathbf{u}_h^0 , and θ_h^0 to be L^2 -orthogonal projection of \mathbf{u}_0 into \mathbf{X}_h , and θ_0 in Y_h , respectively. Select an end time T , and a time step $\Delta t > 0$ such that $T/\Delta t = N$. Then find $(\mathbf{u}_h^{n+1}, p_h^{n+1}, \theta_h^{n+1}) \in (\mathbf{X}_h, Q_h, Y_h)$, $(n = 0, 1, 2, \dots, N-1)$, via the following :

Step 1: Compute $(\tilde{\mathbf{u}}_h^{n+1}, p_h^{n+1}, \tilde{\theta}_h^{n+1}) \in (\mathbf{X}_h, Q_h, Y_h)$ such that for each $(\mathbf{v}_h, q_h, \chi_h) \in (\mathbf{X}_h, Q_h, Y_h)$

$$\begin{aligned} \frac{1}{\Delta t} (\tilde{\mathbf{u}}_h^{n+1} - \mathbf{u}_h^n, \mathbf{v}_h) + \nu (\nabla \tilde{\mathbf{u}}_h^{n+1}, \nabla \mathbf{v}_h) + b(\mathbf{u}_h^n, \tilde{\mathbf{u}}_h^{n+1}, \mathbf{v}_h) - (p_h^{n+1}, \nabla \cdot \mathbf{v}_h) \\ = Ri \left(\langle \mathbf{0}, \tilde{\theta}_h^n \rangle, \mathbf{v}_h \right) + (\mathbf{f}^{n+1}, \mathbf{v}_h), \end{aligned} \quad (3.2)$$

$$(\nabla \cdot \tilde{\mathbf{u}}_h^{n+1}, q_h) = 0, \quad (3.3)$$

$$\frac{1}{\Delta t} (\tilde{\theta}_h^{n+1} - \tilde{\theta}_h^n, \chi_h) + \kappa (\nabla \tilde{\theta}_h^{n+1}, \nabla \chi_h) + b^*(\mathbf{u}_h^n, \tilde{\theta}_h^{n+1}, \chi_h) = (\Psi^{n+1}, \chi_h). \quad (3.4)$$

Step 2: Compute $\mathbf{u}_h^{n+1} \in \mathbf{X}_h$ such that for each $\varphi_h \in \mathbf{X}_h$,

$$(\mathbf{u}_h^{n+1}, \varphi_h) + (\beta + \gamma \Delta t) (\nabla \cdot \mathbf{u}_h^{n+1}, \nabla \cdot \varphi_h) = (\tilde{\mathbf{u}}_h^{n+1}, \varphi_h) + \beta (\nabla \cdot \mathbf{u}_h^n, \nabla \cdot \varphi_h). \quad (3.5)$$

Remark 3.1. We emphasize here that modular grad-div stabilization step can be applied for any multistep time discretization. Numerical analysis for the BDF2 case can be found in [42].

3.1 Stability Analysis

We now focus on the stability of Algorithm 3.1. Our stability analysis shows that approximate solutions of Algorithm 3.1 are stable without any time step restriction. We first present a lemma which gives a relation between the solutions of Step 1 and Step 2, which is necessary for the stability result that follows.

Lemma 3.1. Let \mathbf{u}_h^{n+1} be solutions to (3.5). Then it holds

$$\begin{aligned} \|\tilde{\mathbf{u}}_h^{n+1}\|_{L^2}^2 &= \|\mathbf{u}_h^{n+1}\|_{L^2}^2 + \|\tilde{\mathbf{u}}_h^{n+1} - \mathbf{u}_h^{n+1}\|_{L^2}^2 + 2\gamma \Delta t \|\nabla \cdot \mathbf{u}_h^{n+1}\|_{L^2}^2 \\ &\quad + \beta (\|\nabla \cdot \mathbf{u}_h^{n+1}\|_{L^2}^2 - \|\nabla \cdot \mathbf{u}_h^n\|_{L^2}^2 + \|\nabla \cdot (\mathbf{u}_h^{n+1} - \mathbf{u}_h^n)\|_{L^2}^2). \end{aligned} \quad (3.6)$$

Proof. Set $\varphi_h = \mathbf{u}_h^{n+1}$ in (3.5) which yields

$$(\tilde{\mathbf{u}}_h^{n+1}, \mathbf{u}_h^{n+1}) = \|\mathbf{u}_h^{n+1}\|_{L^2}^2 + (\beta + \gamma \Delta t) \|\nabla \cdot \mathbf{u}_h^{n+1}\|_{L^2}^2 - \beta (\nabla \cdot \mathbf{u}_h^n, \nabla \cdot \mathbf{u}_h^{n+1}). \quad (3.7)$$

Apply the polarization identity on the left hand side and on the last right hand side terms to get:

$$\begin{aligned} (\tilde{\mathbf{u}}_h^{n+1}, \mathbf{u}_h^{n+1}) &= \frac{1}{2} \left(\|\tilde{\mathbf{u}}_h^{n+1}\|_{L^2}^2 + \|\mathbf{u}_h^{n+1}\|_{L^2}^2 - \|\tilde{\mathbf{u}}_h^{n+1} - \mathbf{u}_h^{n+1}\|_{L^2}^2 \right), \\ -\beta (\nabla \cdot \mathbf{u}_h^n, \nabla \cdot \mathbf{u}_h^{n+1}) &= -\frac{\beta}{2} \left(\|\nabla \cdot \mathbf{u}_h^n\|_{L^2}^2 + \|\nabla \cdot \mathbf{u}_h^{n+1}\|_{L^2}^2 - \|\nabla \cdot (\mathbf{u}_h^n - \mathbf{u}_h^{n+1})\|_{L^2}^2 \right). \end{aligned}$$

Inserting these estimates into (3.7), rearranging terms and multiplying by 2 gives the desired estimates. \square

We now present the main stability result.

Lemma 3.2. *Assume that $\mathbf{f} \in L^2(0, T; \mathbf{H}^{-1}(\Omega))$ and $\Psi \in L^2(0, T; H^{-1}(\Omega))$. Then solutions to Algorithm 3.1 satisfy the following: for any $\Delta t > 0$*

$$\begin{aligned} \|\mathbf{u}_h^N\|_{L^2}^2 + \beta \|\nabla \cdot \mathbf{u}_h^N\|_{L^2}^2 + \sum_{n=0}^{N-1} \left(\|\tilde{\mathbf{u}}_h^{n+1} - \mathbf{u}_h^{n+1}\|_{L^2}^2 + \|\tilde{\mathbf{u}}_h^{n+1} - \mathbf{u}_h^n\|_{L^2}^2 \right) + \beta \sum_{n=0}^{N-1} \|\nabla \cdot (\mathbf{u}_h^{n+1} - \mathbf{u}_h^n)\|_{L^2}^2 \\ + 2\gamma \Delta t \sum_{n=0}^{N-1} \|\nabla \cdot \mathbf{u}_h^{n+1}\|_{L^2}^2 + \nu \Delta t \sum_{n=0}^{N-1} \|\nabla \tilde{\mathbf{u}}_h^{n+1}\|_{L^2}^2 \leq 2C_P^2 R t^2 \nu^{-1} T M + 2\nu^{-1} \Delta t \sum_{n=0}^{N-1} \|\mathbf{f}^{n+1}\|_{-1}^2, \end{aligned} \quad (3.8)$$

and

$$\|\tilde{\theta}_h^N\|_{L^2}^2 + \sum_{n=0}^{N-1} \|\tilde{\theta}_h^{n+1} - \tilde{\theta}_h^n\|_{L^2}^2 + \kappa \Delta t \sum_{n=0}^{N-1} \|\nabla \tilde{\theta}_h^{n+1}\|_{L^2}^2 \leq M, \quad (3.9)$$

where $M := \left(\|\tilde{\theta}_h^0\|_{L^2}^2 + \kappa^{-1} \Delta t \sum_{n=0}^{N-1} \|\Psi^{n+1}\|_{-1}^2 \right)$.

Proof. We first prove the temperature stability result. Set $\chi_h = 2\Delta t \tilde{\theta}_h^{n+1}$ in (3.4), which vanishes the non-linear term and leaves:

$$\left(\|\tilde{\theta}_h^{n+1}\|_{L^2}^2 - \|\tilde{\theta}_h^n\|_{L^2}^2 + \|\tilde{\theta}_h^{n+1} - \tilde{\theta}_h^n\|_{L^2}^2 \right) + 2\kappa \Delta t \|\nabla \tilde{\theta}_h^{n+1}\|_{L^2}^2 = 2\Delta t (\Psi^{n+1}, \tilde{\theta}_h^{n+1}).$$

Apply the Cauchy-Schwarz and Young's inequalities on the right hand side term to get

$$2\Delta t (\Psi^{n+1}, \tilde{\theta}_h^{n+1}) \leq \kappa^{-1} \Delta t \|\Psi^{n+1}\|_{-1}^2 + \kappa \Delta t \|\nabla \tilde{\theta}_h^{n+1}\|_{L^2}^2.$$

Inserting this estimate produces

$$\left(\|\tilde{\theta}_h^{n+1}\|_{L^2}^2 - \|\tilde{\theta}_h^n\|_{L^2}^2 + \|\tilde{\theta}_h^{n+1} - \tilde{\theta}_h^n\|_{L^2}^2 \right) + \kappa \Delta t \|\nabla \tilde{\theta}_h^{n+1}\|_{L^2}^2 \leq \kappa^{-1} \Delta t \|\Psi^{n+1}\|_{-1}^2. \quad (3.10)$$

Dropping the non-negative third left hand side term and summing over time steps gives the stability bound for the temperature. For the stability of the velocity, set $(\mathbf{v}_h, q_h) = (2\Delta t \tilde{\mathbf{u}}_h^{n+1}, p_h^{n+1})$ in (3.2)-(3.3) to get

$$\left(\|\tilde{\mathbf{u}}_h^{n+1}\|_{L^2}^2 - \|\mathbf{u}_h^n\|_{L^2}^2 + \|\tilde{\mathbf{u}}_h^{n+1} - \mathbf{u}_h^n\|_{L^2}^2 \right) + 2\nu \Delta t \|\nabla \tilde{\mathbf{u}}_h^{n+1}\|_{L^2}^2 = 2Ri \Delta t \left(\langle 0, \tilde{\theta}_h^n \rangle, \mathbf{v}_h \right) + 2\Delta t (\mathbf{f}^{n+1}, \tilde{\mathbf{u}}_h^{n+1}).$$

Apply the Cauchy-Schwarz and Young's inequalities on the right hand side terms to produce

$$\begin{aligned} 2 \Delta t (\mathbf{f}^{n+1}, \tilde{\mathbf{u}}_h^{n+1}) &\leq 2 \nu^{-1} \Delta t \|\mathbf{f}^{n+1}\|_{-1}^2 + \frac{\nu \Delta t}{2} \|\nabla \tilde{\mathbf{u}}_h^{n+1}\|_{L^2}^2, \\ 2 Ri \Delta t (\langle 0, \tilde{\theta}_h^n \rangle, \mathbf{v}_h) &\leq 2 C_P^2 Ri^2 \nu^{-1} \Delta t \|\tilde{\theta}_h^n\|_{L^2}^2 + \frac{\nu \Delta t}{2} \|\nabla \tilde{\mathbf{u}}_h^{n+1}\|_{L^2}^2. \end{aligned}$$

Insert these estimates and rearrange terms to obtain

$$\left(\|\tilde{\mathbf{u}}_h^{n+1}\|_{L^2}^2 - \|\mathbf{u}_h^n\|_{L^2}^2 + \|\tilde{\mathbf{u}}_h^{n+1} - \mathbf{u}_h^n\|_{L^2}^2 \right) + \nu \Delta t \|\nabla \tilde{\mathbf{u}}_h^{n+1}\|_{L^2}^2 \leq 2 C_P^2 Ri^2 \nu^{-1} \Delta t \|\tilde{\theta}_h^n\|_{L^2}^2 + \frac{\Delta t}{\nu} \|\mathbf{f}^{n+1}\|_{-1}^2.$$

Now use Lemma 3.1 on the left hand side to obtain

$$\begin{aligned} &\left(\|\mathbf{u}_h^{n+1}\|_{L^2}^2 - \|\mathbf{u}_h^n\|_{L^2}^2 \right) + \beta \left(\|\nabla \cdot \mathbf{u}_h^{n+1}\|_{L^2}^2 - \|\nabla \cdot \mathbf{u}_h^n\|_{L^2}^2 \right) + \left(\|\tilde{\mathbf{u}}_h^{n+1} - \mathbf{u}_h^{n+1}\|_{L^2}^2 + \|\tilde{\mathbf{u}}_h^{n+1} - \mathbf{u}_h^n\|_{L^2}^2 \right) \\ &+ \beta \|\nabla \cdot (\mathbf{u}_h^{n+1} - \mathbf{u}_h^n)\|_{L^2}^2 + 2 \gamma \Delta t \|\nabla \cdot \mathbf{u}_h^{n+1}\|_{L^2}^2 + \nu \Delta t \|\nabla \tilde{\mathbf{u}}_h^{n+1}\|_{L^2}^2 \leq 2 C_P^2 Ri^2 \nu^{-1} \Delta t \|\tilde{\theta}_h^n\|_{L^2}^2 + \nu^{-1} \Delta t \|\mathbf{f}^{n+1}\|_{-1}^2. \end{aligned}$$

Notice that from (3.10), one can get

$$\Delta t \sum_{n=0}^{N-1} \|\tilde{\theta}_h^n\|_{L^2}^2 \leq \Delta t N \left(\|\tilde{\theta}_h^0\|_{L^2}^2 + \kappa^{-1} \Delta t \sum_{n=0}^{N-1} \|\Psi_h^{n+1}\|_{-1}^2 \right) =: T M.$$

Summing over time steps with this estimate and rearranging terms finishes the proof. \square

3.2 Error Analysis

In this section, we show that solutions of the proposed algorithm converge to the true solution, and that convergence is optimal provided $\Delta t \leq h$. We denote the true Boussinesq solution at time level $(n+1)$ by

$$\mathbf{u}^{n+1} := \mathbf{u}(t^{n+1}), \quad p^{n+1} := p(t^{n+1}), \quad \theta^{n+1} := \theta(t^{n+1}).$$

The error analysis needs the following error decompositions at each time level:

$$\begin{aligned} \mathbf{e}_u^{n+1} &:= \mathbf{u}^{n+1} - \tilde{\mathbf{u}}_h^{n+1} = (\mathbf{u}^{n+1} - \mathbf{P}_{\mathbf{V}_h}(\mathbf{u}^{n+1})) - (\tilde{\mathbf{u}}_h^{n+1} - \mathbf{P}_{\mathbf{V}_h}(\mathbf{u}^{n+1})) =: \boldsymbol{\eta}_{\mathbf{u}}^{n+1} - \boldsymbol{\Lambda}_{\mathbf{u},h}^{n+1}, \\ \mathbf{e}_u^{n+1} &:= \mathbf{u}^{n+1} - \mathbf{u}_h^{n+1} = (\mathbf{u}^{n+1} - \mathbf{P}_{\mathbf{V}_h}(\mathbf{u}^{n+1})) - (\mathbf{u}_h^{n+1} - \mathbf{P}_{\mathbf{V}_h}(\mathbf{u}^{n+1})) =: \boldsymbol{\eta}_{\mathbf{u}}^{n+1} - \boldsymbol{\phi}_{\mathbf{u},h}^{n+1}, \\ e_\theta^{n+1} &:= \theta^{n+1} - \tilde{\theta}_h^{n+1} = (\theta^{n+1} - P_{Y_h}(\theta^{n+1})) - (\tilde{\theta}_h^{n+1} - P_{Y_h}(\theta^{n+1})) =: \eta_\theta^{n+1} - \Lambda_{\theta,h}^{n+1}, \end{aligned}$$

where $\mathbf{P}_{\mathbf{V}_h}(\mathbf{u}^{n+1})$ is the L^2 -best approximation of \mathbf{u}^{n+1} in \mathbf{V}_h , and $P_{Y_h}(\theta^{n+1})$ the L^2 -best approximation of θ^{n+1} in Y_h . Moreover, $\boldsymbol{\eta}_{\mathbf{u}}^{n+1}$, η_θ^{n+1} are interpolation errors, and $\boldsymbol{\Lambda}_{\mathbf{u},h}^{n+1}$, $\boldsymbol{\phi}_{\mathbf{u},h}^{n+1} \in \mathbf{X}_h$ and $\Lambda_{\theta,h}^{n+1} \in Y_h$ are finite element errors. We now present the following result which helps us to prove the convergence theorem.

Lemma 3.3. *Consider the second step of Algorithm 3.1. Then it holds:*

$$\begin{aligned} \|\boldsymbol{\Lambda}_{\mathbf{u},h}^{n+1}\|_{L^2}^2 &\geq \|\boldsymbol{\phi}_{\mathbf{u},h}^{n+1}\|_{L^2}^2 + \|\boldsymbol{\Lambda}_{\mathbf{u},h}^{n+1} - \boldsymbol{\phi}_{\mathbf{u},h}^{n+1}\|_{L^2}^2 + \beta \left(\|\nabla \cdot \boldsymbol{\phi}_{\mathbf{u},h}^{n+1}\|_{L^2}^2 - \|\nabla \cdot \boldsymbol{\phi}_{\mathbf{u},h}^n\|_{L^2}^2 \right) \\ &+ \frac{\beta}{2} \|\nabla \cdot (\boldsymbol{\phi}_{\mathbf{u},h}^{n+1} - \boldsymbol{\phi}_{\mathbf{u},h}^n)\|_{L^2}^2 + \gamma \Delta t \|\nabla \cdot \boldsymbol{\phi}_{\mathbf{u},h}^{n+1}\|_{L^2}^2 - \beta \Delta t \|\nabla \cdot \boldsymbol{\phi}_{\mathbf{u},h}^n\|_{L^2}^2 \\ &- \beta (1 + 2 \Delta t) \|\nabla \boldsymbol{\eta}_{\mathbf{u},t}\|_{L^2(t^n, t^{n+1}; L^2(\Omega))}^2 - \gamma \Delta t \|\nabla \boldsymbol{\eta}_{\mathbf{u}}^{n+1}\|_{L^2}^2. \end{aligned}$$

Proof. The true velocity solution at time level $(n+1)$ satisfies the following:

$$(\mathbf{u}^{n+1}, \mathbf{v}_h) + (\beta + \gamma \Delta t)(\nabla \cdot \mathbf{u}^{n+1}, \nabla \cdot \mathbf{v}_h) = (\mathbf{u}^{n+1}, \mathbf{v}_h) + \beta(\nabla \cdot \mathbf{u}^n, \nabla \cdot \mathbf{v}_h).$$

Subtract this system from the second step of Algorithm 3.1. Then using error notation and rearranging terms produces

$$(\mathbf{e}_{\mathbf{u}}^{n+1}, \mathbf{v}_h) + \beta(\nabla \cdot (\mathbf{e}_{\mathbf{u}}^{n+1} - \mathbf{e}_{\mathbf{u}}^n), \nabla \cdot \mathbf{v}_h) + \gamma \Delta t (\nabla \cdot \mathbf{e}_{\mathbf{u}}^{n+1}, \nabla \cdot \mathbf{v}_h) = (\mathbf{e}_{\mathbf{u}}^{n+1}, \mathbf{v}_h).$$

Using error decomposition and setting $\mathbf{v}_h = \phi_{\mathbf{u},h}^{n+1}$ yields

$$\begin{aligned} & \|\phi_{\mathbf{u},h}^{n+1}\|_{L^2}^2 + \frac{\beta}{2} (\|\nabla \cdot \phi_{\mathbf{u},h}^{n+1}\|_{L^2}^2 - \|\nabla \cdot \phi_{\mathbf{u},h}^n\|_{L^2}^2 + \|\nabla \cdot (\phi_{\mathbf{u},h}^{n+1} - \phi_{\mathbf{u},h}^n)\|_{L^2}^2) + \gamma \Delta t \|\nabla \cdot \phi_{\mathbf{u},h}^{n+1}\|_{L^2}^2 \\ &= (\eta_{\mathbf{u}}^{n+1}, \phi_{\mathbf{u},h}^{n+1}) + \beta(\nabla \cdot (\eta_{\mathbf{u}}^{n+1} - \eta_{\mathbf{u}}^n), \nabla \cdot \phi_{\mathbf{u},h}^{n+1}) + \gamma \Delta t (\nabla \cdot \eta_{\mathbf{u}}^{n+1}, \nabla \cdot \phi_{\mathbf{u},h}^{n+1}) - (\eta_{\mathbf{u}}^{n+1} - \Lambda_{\mathbf{u},h}^{n+1}, \phi_{\mathbf{u},h}^{n+1}). \end{aligned}$$

Now add $\mp \beta(\nabla \cdot (\eta_{\mathbf{u}}^{n+1} - \eta_{\mathbf{u}}^n), \nabla \cdot \phi_{\mathbf{u},h}^n)$ and notice that $(\eta_{\mathbf{u}}^{n+1}, \phi_{\mathbf{u},h}^{n+1}) = 0$. This produces

$$\begin{aligned} & \|\phi_{\mathbf{u},h}^{n+1}\|_{L^2}^2 + \frac{\beta}{2} (\|\nabla \cdot \phi_{\mathbf{u},h}^{n+1}\|_{L^2}^2 - \|\nabla \cdot \phi_{\mathbf{u},h}^n\|_{L^2}^2 + \|\nabla \cdot (\phi_{\mathbf{u},h}^{n+1} - \phi_{\mathbf{u},h}^n)\|_{L^2}^2) + \gamma \Delta t \|\nabla \cdot \phi_{\mathbf{u},h}^{n+1}\|_{L^2}^2 \\ &= \beta(\nabla \cdot (\eta_{\mathbf{u}}^{n+1} - \eta_{\mathbf{u}}^n), \nabla \cdot (\phi_{\mathbf{u},h}^{n+1} - \phi_{\mathbf{u},h}^n)) + \beta(\nabla \cdot (\eta_{\mathbf{u}}^{n+1} - \eta_{\mathbf{u}}^n), \nabla \cdot \phi_{\mathbf{u},h}^n) \\ &\quad + \gamma \Delta t (\nabla \cdot \eta_{\mathbf{u}}^{n+1}, \nabla \cdot \phi_{\mathbf{u},h}^{n+1}) + (\Lambda_{\mathbf{u},h}^{n+1}, \phi_{\mathbf{u},h}^{n+1}). \end{aligned}$$

To bound the first three right hand side terms, apply the Cauchy-Schwarz, and the Young's inequalities to get

$$\begin{aligned} \beta(\nabla \cdot (\eta_{\mathbf{u}}^{n+1} - \eta_{\mathbf{u}}^n), \nabla \cdot (\phi_{\mathbf{u},h}^{n+1} - \phi_{\mathbf{u},h}^n)) &\leq \beta \|\nabla(\eta_{\mathbf{u}}^{n+1} - \eta_{\mathbf{u}}^n)\|_{L^2} \|\nabla \cdot (\phi_{\mathbf{u},h}^{n+1} - \phi_{\mathbf{u},h}^n)\|_{L^2} \\ &\leq \beta \Delta t \|\nabla \eta_{\mathbf{u},t}\|_{L^2(t^n, t^{n+1}; L^2(\Omega))}^2 + \frac{\beta}{4} \|\nabla \cdot (\phi_{\mathbf{u},h}^{n+1} - \phi_{\mathbf{u},h}^n)\|_{L^2}^2, \\ \beta(\nabla \cdot (\eta_{\mathbf{u}}^{n+1} - \eta_{\mathbf{u}}^n), \nabla \cdot \phi_{\mathbf{u},h}^n) &\leq \beta \|\nabla(\eta_{\mathbf{u}}^{n+1} - \eta_{\mathbf{u}}^n)\|_{L^2} \|\nabla \cdot \phi_{\mathbf{u},h}^n\|_{L^2} \\ &\leq \frac{\beta}{2} \|\nabla \eta_{\mathbf{u},t}\|_{L^2(t^n, t^{n+1}; L^2(\Omega))}^2 + \frac{\beta \Delta t}{2} \|\nabla \cdot \phi_{\mathbf{u},h}^n\|_{L^2}^2, \\ \gamma \Delta t (\nabla \cdot \eta_{\mathbf{u}}^{n+1}, \nabla \cdot \phi_{\mathbf{u},h}^{n+1}) &\leq \gamma \Delta t \|\nabla \eta_{\mathbf{u}}^{n+1}\|_{L^2} \|\nabla \cdot \phi_{\mathbf{u},h}^{n+1}\|_{L^2} \leq \frac{\gamma \Delta t}{2} \|\nabla \eta_{\mathbf{u}}^{n+1}\|_{L^2}^2 + \frac{\gamma \Delta t}{2} \|\nabla \cdot \phi_{\mathbf{u},h}^{n+1}\|_{L^2}^2. \end{aligned}$$

For the last term, use the polarization identity to obtain

$$(\Lambda_{\mathbf{u},h}^{n+1}, \phi_{\mathbf{u},h}^{n+1}) = \frac{1}{2} (\|\Lambda_{\mathbf{u},h}^{n+1}\|_{L^2}^2 + \|\phi_{\mathbf{u},h}^{n+1}\|_{L^2}^2 - \|\Lambda_{\mathbf{u},h}^{n+1} - \phi_{\mathbf{u},h}^{n+1}\|_{L^2}^2).$$

Plugging these estimates into velocity error equation, and reducing yields

$$\begin{aligned} & \frac{1}{2} \|\phi_{\mathbf{u},h}^{n+1}\|_{L^2}^2 + \frac{\beta}{2} (\|\nabla \cdot \phi_{\mathbf{u},h}^{n+1}\|_{L^2}^2 - \|\nabla \cdot \phi_{\mathbf{u},h}^n\|_{L^2}^2) + \frac{\beta}{4} \|\nabla \cdot (\phi_{\mathbf{u},h}^{n+1} - \phi_{\mathbf{u},h}^n)\|_{L^2}^2 + \frac{\gamma \Delta t}{2} \|\nabla \cdot \phi_{\mathbf{u},h}^{n+1}\|_{L^2}^2 \\ &\leq \frac{\beta (1 + 2\Delta t)}{2} \|\nabla \eta_{\mathbf{u},t}\|_{L^2(t^n, t^{n+1}; L^2(\Omega))}^2 + \frac{\beta \Delta t}{2} \|\nabla \cdot \phi_{\mathbf{u},h}^n\|_{L^2}^2 + \frac{\gamma \Delta t}{2} \|\nabla \eta_{\mathbf{u}}^{n+1}\|_{L^2}^2 \\ &\quad + \frac{1}{2} (\|\Lambda_{\mathbf{u},h}^{n+1}\|_{L^2}^2 - \|\Lambda_{\mathbf{u},h}^{n+1} - \phi_{\mathbf{u},h}^{n+1}\|_{L^2}^2). \end{aligned}$$

Multiplying by $2\Delta t$, and rearranging terms gives the desired estimate. \square

We now prove an error estimate to Algorithm 3.1.

Theorem 3.1. *Assume that true solution (\mathbf{u}, θ, p) satisfies the regularity conditions :*

$$\begin{aligned} \mathbf{u}, \mathbf{u}_t &\in L^\infty(0, T; \mathbf{H}^{k+1}(\Omega)), \quad \mathbf{u}_{tt} \in L^2(0, T; L^2(\Omega)), \\ p &\in L^\infty(0, T; L^2(\Omega)), \\ \theta, \theta_t &\in L^\infty(0, T; H^{k+1}(\Omega)), \quad \theta_t, \theta_{tt} \in L^2(0, T; L^2(\Omega)). \end{aligned}$$

Let $(\tilde{\mathbf{u}}_h^{n+1}, p_h^{n+1}, \tilde{\theta}_h^{n+1}, \mathbf{u}_h^{n+1})$ be solution to Algorithm 3.1, and (\mathbf{X}_h, Q_h, Y_h) is given by $(\mathbf{P}_k, P_{k-1}, P_k)$. Then the errors satisfy the bound:

$$\begin{aligned} \|\mathbf{e}_{\mathbf{u}}^N\|_{L^2}^2 + \|\mathbf{e}_{\tilde{\theta}}^N\|_{L^2}^2 + \beta \|\nabla \cdot \mathbf{e}_{\mathbf{u}}^N\|_{L^2}^2 + \gamma \|\nabla \cdot \mathbf{e}_{\mathbf{u}}\|_{2,0}^2 + \nu \|\nabla \mathbf{e}_{\tilde{\mathbf{u}}}\|_{2,0}^2 + \kappa \|\nabla \mathbf{e}_{\tilde{\theta}}\|_{2,0}^2 \\ \leq C (h^{2k+2} + \Delta t h^{2k-1} + h^{2k} + \Delta t^2), \end{aligned} \quad (3.11)$$

where C is a generic constant independent of the time step and mesh size.

Proof. The proof is divided into four steps since it is very long and technical. In the first step, the error equations are obtained by splitting the velocity and magnetic errors into approximation errors and finite element remainders. In the second step, all right hand side terms of the error equations are bounded below. The third step applies the discrete Gronwall lemma, and the last step the triangle inequality for the error terms.

Step 1: The derivation of error equations True solution (\mathbf{u}, p, θ) satisfies the equations:

$$\begin{aligned} \left(\frac{\mathbf{u}^{n+1} - \mathbf{u}^n}{\Delta t}, \mathbf{v}_h \right) + \nu (\nabla \mathbf{u}^{n+1}, \nabla \mathbf{v}_h) + b(\mathbf{u}^n, \mathbf{u}^{n+1}, \mathbf{v}_h) - (p^{n+1}, \nabla \cdot \mathbf{v}_h) = Ri(\langle 0, \theta^n \rangle, \mathbf{v}_h) \\ + (\mathbf{f}^{n+1}, \mathbf{v}_h) - E_1(\mathbf{u}, \theta, \mathbf{v}_h), \end{aligned} \quad (3.12)$$

$$\left(\frac{\theta^{n+1} - \theta^n}{\Delta t}, \chi_h \right) + \kappa (\nabla \theta^{n+1}, \nabla \chi_h) + b^*(\mathbf{u}^n, \theta^{n+1}, \chi_h) = (\Psi^{n+1}, \chi_h) - E_2(\mathbf{u}, \theta, \chi_h), \quad (3.13)$$

where $E_1(\mathbf{u}, \theta, \mathbf{v}_h)$ and $E_2(\mathbf{u}, \theta, \chi_h)$ are consistency errors and given by

$$\begin{aligned} E_1(\mathbf{u}, \theta, \mathbf{v}_h) &:= \left(\mathbf{u}_t^{n+1} - \frac{\mathbf{u}^{n+1} - \mathbf{u}^n}{\Delta t}, \mathbf{v}_h \right) + b(\mathbf{u}^{n+1} - \mathbf{u}^n, \mathbf{u}^{n+1}, \mathbf{v}_h) - Ri(\langle 0, \theta^{n+1} - \theta^n \rangle, \mathbf{v}_h) \\ E_2(\mathbf{u}, \theta, \chi_h) &:= \left(\theta_t^{n+1} - \frac{\theta^{n+1} - \theta^n}{\Delta t}, \chi_h \right) + b^*(\mathbf{u}^{n+1} - \mathbf{u}^n, \theta^{n+1}, \chi_h). \end{aligned}$$

Subtract the first step of Algorithm 3.1 from (3.12)-(3.13), and use error notation to produce

$$\begin{aligned} \left(\frac{\mathbf{e}_{\tilde{\mathbf{u}}}^{n+1} - \mathbf{e}_{\tilde{\mathbf{u}}}^n}{\Delta t}, \mathbf{v}_h \right) + \nu (\nabla \mathbf{e}_{\tilde{\mathbf{u}}}^{n+1}, \nabla \mathbf{v}_h) + b(\mathbf{u}^n, \mathbf{u}^{n+1}, \mathbf{v}_h) - b(\mathbf{u}_h^n, \tilde{\mathbf{u}}_h^{n+1}, \mathbf{v}_h) - (p^{n+1} - p_h^{n+1}, \nabla \cdot \mathbf{v}_h) \\ - Ri(\langle 0, e_{\tilde{\theta}}^n \rangle, \mathbf{v}_h) + E_1(\mathbf{u}, \theta, \mathbf{v}_h) = 0, \end{aligned} \quad (3.14)$$

and

$$\left(\frac{e_{\tilde{\theta}}^{n+1} - e_{\tilde{\theta}}^n}{\Delta t}, \chi_h \right) + \kappa (\nabla e_{\tilde{\theta}}^{n+1}, \nabla \chi_h) + b^*(\mathbf{u}^n, \theta^{n+1}, \chi_h) - b^*(\mathbf{u}_h^n, \tilde{\theta}_h^{n+1}, \chi_h) + E_2(\mathbf{u}, \theta, \chi_h) = 0. \quad (3.15)$$

Using error decomposition and setting $\mathbf{v}_h = 2\Delta t \mathbf{\Lambda}_{\mathbf{u},h}^{n+1}$ in (3.14), and $\chi_h = 2\Delta t \mathbf{\Lambda}_{\theta,h}^{n+1}$ in (3.15) yields: for any $q_h \in Q_h$,

$$\begin{aligned} \|\mathbf{\Lambda}_{\mathbf{u},h}^{n+1}\|_{L^2}^2 - \|\phi_{\mathbf{u},h}^n\|_{L^2}^2 + \|\mathbf{\Lambda}_{\mathbf{u},h}^{n+1} - \phi_{\mathbf{u},h}^n\|_{L^2}^2 + 2\nu\Delta t \|\nabla \mathbf{\Lambda}_{\mathbf{u},h}^{n+1}\|_{L^2}^2 \\ = 2 \left(\eta_{\mathbf{u}}^{n+1} - \eta_{\mathbf{u}}^n, \mathbf{\Lambda}_{\mathbf{u},h}^{n+1} \right) + 2\nu\Delta t \left(\nabla \eta_{\mathbf{u}}^{n+1}, \nabla \mathbf{\Lambda}_{\mathbf{u},h}^{n+1} \right) + 2\Delta t \left(b(\mathbf{u}^n, \mathbf{u}^{n+1}, \mathbf{\Lambda}_{\mathbf{u},h}^{n+1}) - b(\mathbf{u}_h^n, \tilde{\mathbf{u}}_h^{n+1}, \mathbf{\Lambda}_{\mathbf{u},h}^{n+1}) \right) \\ - 2 Ri \Delta t \langle \langle 0, e_{\tilde{\theta}}^n \rangle, \mathbf{\Lambda}_{\mathbf{u},h}^{n+1} \rangle - 2 \Delta t \left(p^{n+1} - q_h, \nabla \cdot \mathbf{\Lambda}_{\mathbf{u},h}^{n+1} \right) + 2 \Delta t E_1(\mathbf{u}, \theta, \mathbf{\Lambda}_{\mathbf{u},h}^{n+1}), \end{aligned} \quad (3.16)$$

and

$$\begin{aligned}
& \|\Lambda_{\theta,h}^{n+1}\|_{L^2}^2 - \|\Lambda_{\theta,h}^n\|_{L^2}^2 + \|\Lambda_{\theta,h}^{n+1} - \Lambda_{\theta,h}^n\|_{L^2}^2 + 2\kappa\Delta t \|\nabla \Lambda_{\theta,h}^{n+1}\|_{L^2}^2 \\
& = 2 \left(\eta_{\theta}^{n+1} - \eta_{\theta}^n, \Lambda_{\theta,h}^{n+1} \right) + 2\kappa\Delta t \left(\nabla \eta_{\theta}^{n+1}, \nabla \Lambda_{\theta,h}^{n+1} \right) + 2\Delta t \left(b^*(\mathbf{u}^n, \theta^{n+1}, \Lambda_{\theta,h}^{n+1}) - b^*(\mathbf{u}_h^n, \tilde{\theta}_h^{n+1}, \Lambda_{\theta,h}^{n+1}) \right) \\
& \quad + 2\Delta t E_2(\mathbf{u}, \theta, \Lambda_{\theta,h}^{n+1}). \quad (3.17)
\end{aligned}$$

Now rewrite the first two linear terms in Equation 3.16: first add $\pm b(\mathbf{u}_h^n, \mathbf{u}^{n+1}, \Lambda_{\mathbf{u},h}^{n+1})$ and notice that $b(\mathbf{u}_h^n, \Lambda_{\mathbf{u},h}^{n+1}, \Lambda_{\mathbf{u},h}^{n+1}) = 0$, then add $\mp b(\tilde{\mathbf{u}}_h^{n+1}, \boldsymbol{\eta}_{\mathbf{u}}^{n+1}, \Lambda_{\mathbf{u},h}^{n+1})$ to get

$$\begin{aligned}
b(\mathbf{u}^n, \mathbf{u}^{n+1}, \Lambda_{\mathbf{u},h}^{n+1}) & - b(\mathbf{u}_h^n, \mathbf{u}^{n+1}, \Lambda_{\mathbf{u},h}^{n+1}) + b(\mathbf{u}_h^n, \mathbf{u}^{n+1}, \Lambda_{\mathbf{u},h}^{n+1}) - b(\mathbf{u}_h^n, \tilde{\mathbf{u}}_h^{n+1}, \Lambda_{\mathbf{u},h}^{n+1}) \\
& = b(\mathbf{e}_{\mathbf{u}}^n, \mathbf{u}^{n+1}, \Lambda_{\mathbf{u},h}^{n+1}) + b(\mathbf{u}_h^n, \mathbf{e}_{\tilde{\mathbf{u}}}^{n+1}, \Lambda_{\mathbf{u},h}^{n+1}) \\
& = b(\mathbf{e}_{\mathbf{u}}^n, \mathbf{u}^{n+1}, \Lambda_{\mathbf{u},h}^{n+1}) + b(\mathbf{u}_h^n, \boldsymbol{\eta}_{\mathbf{u}}^{n+1}, \Lambda_{\mathbf{u},h}^{n+1}), -b(\tilde{\mathbf{u}}_h^{n+1}, \boldsymbol{\eta}_{\mathbf{u}}^{n+1}, \Lambda_{\mathbf{u},h}^{n+1}) + b(\tilde{\mathbf{u}}_h^{n+1}, \boldsymbol{\eta}_{\mathbf{u}}^{n+1}, \Lambda_{\mathbf{u},h}^{n+1}) \\
& = b(\mathbf{e}_{\mathbf{u}}^n, \mathbf{u}^{n+1}, \Lambda_{\mathbf{u},h}^{n+1}) + b(\mathbf{u}_h^n - \tilde{\mathbf{u}}_h^{n+1}, \boldsymbol{\eta}_{\mathbf{u}}^{n+1}, \Lambda_{\mathbf{u},h}^{n+1}) + b(\tilde{\mathbf{u}}_h^{n+1}, \boldsymbol{\eta}_{\mathbf{u}}^{n+1}, \Lambda_{\mathbf{u},h}^{n+1}).
\end{aligned}$$

Inserting these, Equation 3.16 becomes

$$\begin{aligned}
& \|\Lambda_{\mathbf{u},h}^{n+1}\|_{L^2}^2 - \|\phi_{\mathbf{u},h}^n\|_{L^2}^2 + \|\Lambda_{\mathbf{u},h}^{n+1} - \phi_{\mathbf{u},h}^n\|_{L^2}^2 + 2\nu\Delta t \|\nabla \Lambda_{\mathbf{u},h}^{n+1}\|_{L^2}^2 \\
& = 2 \left(\boldsymbol{\eta}_{\mathbf{u}}^{n+1} - \boldsymbol{\eta}_{\mathbf{u}}^n, \Lambda_{\mathbf{u},h}^{n+1} \right) + 2\nu\Delta t \left(\nabla \boldsymbol{\eta}_{\mathbf{u}}^{n+1}, \nabla \Lambda_{\mathbf{u},h}^{n+1} \right) + 2\Delta t \left(b(\mathbf{e}_{\mathbf{u}}^n, \mathbf{u}^{n+1}, \Lambda_{\mathbf{u},h}^{n+1}) + b(\mathbf{u}_h^n - \tilde{\mathbf{u}}_h^{n+1}, \boldsymbol{\eta}_{\mathbf{u}}^{n+1}, \Lambda_{\mathbf{u},h}^{n+1}) \right) \\
& \quad + 2\Delta t b(\tilde{\mathbf{u}}_h^{n+1}, \boldsymbol{\eta}_{\mathbf{u}}^{n+1}, \Lambda_{\mathbf{u},h}^{n+1}) - 2Ri\Delta t (\langle \mathbf{0}, e_{\theta}^n \rangle, \Lambda_{\mathbf{u},h}^{n+1}) - 2\Delta t \left(p^{n+1} - q_h, \nabla \cdot \Lambda_{\mathbf{u},h}^{n+1} \right) \\
& \quad + 2\Delta t E_1(\mathbf{u}, \theta, \Lambda_{\mathbf{u},h}^{n+1}). \quad (3.18)
\end{aligned}$$

Using similar ideas for the nonlinear terms in Equation 3.17 yields

$$\begin{aligned}
& \|\Lambda_{\theta,h}^{n+1}\|_{L^2}^2 - \|\Lambda_{\theta,h}^n\|_{L^2}^2 + \|\Lambda_{\theta,h}^{n+1} - \Lambda_{\theta,h}^n\|_{L^2}^2 + 2\kappa\Delta t \|\nabla \Lambda_{\theta,h}^{n+1}\|_{L^2}^2 \\
& = 2 \left(\eta_{\theta}^{n+1} - \eta_{\theta}^n, \Lambda_{\theta,h}^{n+1} \right) + 2\kappa\Delta t \left(\nabla \eta_{\theta}^{n+1}, \nabla \Lambda_{\theta,h}^{n+1} \right) \\
& + 2\Delta t \left(b^*(\mathbf{e}_{\mathbf{u}}^n, \theta^{n+1}, \Lambda_{\theta,h}^{n+1}) + b^*(\mathbf{u}_h^n - \tilde{\mathbf{u}}_h^{n+1}, \eta_{\theta}^{n+1}, \Lambda_{\theta,h}^{n+1}) + b^*(\tilde{\mathbf{u}}_h^{n+1}, \eta_{\theta}^{n+1}, \Lambda_{\theta,h}^{n+1}) \right) + 2\Delta t E_2(\mathbf{u}, \theta, \Lambda_{\theta,h}^{n+1}). \quad (3.19)
\end{aligned}$$

Step 2: The estimation of the right hand side terms of error equations

We note that right hand side terms of Equation (3.18)-(3.19) are bounded in a similar way. Therefore, we only give estimates of the right hand side terms for Equation (3.18). To bound the first term in (3.18), one can apply the estimate of the dual pairing, and Young's inequality while for the second one, the Cauchy-Schwarz and Young's inequalities :

$$\begin{aligned}
2 \left(\boldsymbol{\eta}_{\mathbf{u}}^{n+1} - \boldsymbol{\eta}_{\mathbf{u}}^n, \Lambda_{\mathbf{u},h}^{n+1} \right) & \leq \frac{1}{\varepsilon_1} \|\boldsymbol{\eta}_{\mathbf{u},t}\|_{L^2(t^n, t^{n+1}; H^{-1}(\Omega))}^2 + \varepsilon_1 \Delta t \|\nabla \Lambda_{\mathbf{u},h}^{n+1}\|_{L^2}^2, \\
2\nu\Delta t \left(\nabla \boldsymbol{\eta}_{\mathbf{u}}^{n+1}, \nabla \Lambda_{\mathbf{u},h}^{n+1} \right) & \leq \frac{\nu\Delta t}{\varepsilon_2} \|\nabla \boldsymbol{\eta}_{\mathbf{u}}^{n+1}\|_{L^2}^2 + \varepsilon_2 \nu \Delta t \|\nabla \Lambda_{\mathbf{u},h}^{n+1}\|_{L^2}^2.
\end{aligned}$$

For the first non linear term, we first use the error decomposition

$$2\Delta t b(\mathbf{e}_{\mathbf{u}}^n, \mathbf{u}^{n+1}, \Lambda_{\mathbf{u},h}^{n+1}) = 2\Delta t b(\boldsymbol{\eta}_{\mathbf{u}}^n, \mathbf{u}^{n+1}, \Lambda_{\mathbf{u},h}^{n+1}) - 2\Delta t b(\phi_{\mathbf{u},h}^n, \mathbf{u}^{n+1}, \Lambda_{\mathbf{u},h}^{n+1}).$$

For the first term, apply the second estimate of Lemma 2.1 together with the Young's inequality to obtain

$$\begin{aligned} 2 \Delta t b(\boldsymbol{\eta}_{\mathbf{u}}^n, \mathbf{u}^{n+1}, \boldsymbol{\Lambda}_{\mathbf{u},h}^{n+1}) &\leq 2 C \Delta t \sqrt{\|\boldsymbol{\eta}_{\mathbf{u}}^n\|_{L^2} \|\nabla \boldsymbol{\eta}_{\mathbf{u}}^n\|_{L^2}} \|\nabla \mathbf{u}^{n+1}\|_{L^2} \|\nabla \boldsymbol{\Lambda}_{\mathbf{u},h}^{n+1}\|_{L^2} \\ &\leq \frac{C \Delta t}{\varepsilon_3} \|\nabla \mathbf{u}^{n+1}\|_{L^2}^2 \|\boldsymbol{\eta}_{\mathbf{u}}^n\|_{L^2} \|\nabla \boldsymbol{\eta}_{\mathbf{u}}^n\|_{L^2} + \varepsilon_3 \Delta t \|\nabla \boldsymbol{\Lambda}_{\mathbf{u},h}^{n+1}\|_{L^2}^2. \end{aligned}$$

The second term is first expanded by using the definition of $b(\cdot, \cdot, \cdot)$, and then it is applied the Hölder inequality with $L^3 - L^2 - L^6$ on the first and $L^2 - L^\infty - L^2$ on the second, and the Sobolev embedding theorem together with the Poincare and Young's inequalities:

$$\begin{aligned} 2 \Delta t b(\boldsymbol{\phi}_{\mathbf{u},h}^n, \mathbf{u}^{n+1}, \boldsymbol{\Lambda}_{\mathbf{u},h}^{n+1}) &= 2 \Delta t \left((\boldsymbol{\phi}_{\mathbf{u},h}^n \cdot \nabla \mathbf{u}^{n+1}, \boldsymbol{\Lambda}_{\mathbf{u},h}^{n+1}) + \frac{1}{2} ((\nabla \cdot \boldsymbol{\phi}_{\mathbf{u},h}^n) \mathbf{u}^{n+1}, \boldsymbol{\Lambda}_{\mathbf{u},h}^{n+1}) \right) \\ &\leq 2 \Delta t \|\boldsymbol{\phi}_{\mathbf{u},h}^n\|_{L^2} \|\nabla \mathbf{u}^{n+1}\|_{L^3} \|\boldsymbol{\Lambda}_{\mathbf{u},h}^{n+1}\|_{L^6} + \Delta t \|\nabla \cdot \boldsymbol{\phi}_{\mathbf{u},h}^n\|_{L^2} \|\mathbf{u}^{n+1}\|_{L^\infty} \|\boldsymbol{\Lambda}_{\mathbf{u},h}^{n+1}\|_{L^2} \\ &\leq 2 C \Delta t \|\boldsymbol{\phi}_{\mathbf{u},h}^n\|_{L^2} \|\nabla \mathbf{u}^{n+1}\|_{L^3} \|\nabla \boldsymbol{\Lambda}_{\mathbf{u},h}^{n+1}\|_{L^2} + C_P \Delta t \|\nabla \cdot \boldsymbol{\phi}_{\mathbf{u},h}^n\|_{L^2} \|\mathbf{u}^{n+1}\|_{L^\infty} \|\nabla \boldsymbol{\Lambda}_{\mathbf{u},h}^{n+1}\|_{L^2} \\ &\leq \frac{C \Delta t}{\varepsilon_4} \|\nabla \mathbf{u}^{n+1}\|_{L^3}^2 \|\boldsymbol{\phi}_{\mathbf{u},h}^n\|_{L^2}^2 + \frac{C_P^2 \Delta t}{2 \varepsilon_5} \|\mathbf{u}^{n+1}\|_{L^\infty}^2 \|\nabla \cdot \boldsymbol{\phi}_{\mathbf{u},h}^n\|_{L^2}^2 + (\varepsilon_4 + \varepsilon_5/2) \Delta t \|\nabla \boldsymbol{\Lambda}_{\mathbf{u},h}^{n+1}\|_{L^2}^2. \end{aligned}$$

For $b(\mathbf{u}_h^n - \tilde{\mathbf{u}}_h^{n+1}, \boldsymbol{\eta}_{\mathbf{u}}^{n+1}, \boldsymbol{\Lambda}_{\mathbf{u},h}^{n+1})$, we apply Lemma 2.1 together with the inverse inequality, and for $b(\tilde{\mathbf{u}}_h^{n+1}, \boldsymbol{\eta}_{\mathbf{u}}^{n+1}, \boldsymbol{\Lambda}_{\mathbf{u},h}^{n+1})$ Lemma 2.1 to get

$$\begin{aligned} 2 \Delta t b(\mathbf{u}_h^n - \tilde{\mathbf{u}}_h^{n+1}, \boldsymbol{\eta}_{\mathbf{u}}^{n+1}, \boldsymbol{\Lambda}_{\mathbf{u},h}^{n+1}) &\leq 2 C \Delta t \sqrt{\|\mathbf{u}_h^n - \tilde{\mathbf{u}}_h^{n+1}\|_{L^2} \|\nabla (\mathbf{u}_h^n - \tilde{\mathbf{u}}_h^{n+1})\|_{L^2}} \|\nabla \boldsymbol{\eta}_{\mathbf{u}}^{n+1}\|_{L^2} \|\nabla \boldsymbol{\Lambda}_{\mathbf{u},h}^{n+1}\|_{L^2} \\ &\leq 2 C \Delta t h^{-1/2} \|\mathbf{u}_h^n - \tilde{\mathbf{u}}_h^{n+1}\|_{L^2} \|\nabla \boldsymbol{\eta}_{\mathbf{u}}^{n+1}\|_{L^2} \|\nabla \boldsymbol{\Lambda}_{\mathbf{u},h}^{n+1}\|_{L^2} \\ &\leq \frac{C \Delta t h^{-1}}{\varepsilon_6} \|\mathbf{u}_h^n - \tilde{\mathbf{u}}_h^{n+1}\|_{L^2}^2 \|\nabla \boldsymbol{\eta}_{\mathbf{u}}^{n+1}\|_{L^2}^2 + \varepsilon_6 \Delta t \|\nabla \boldsymbol{\Lambda}_{\mathbf{u},h}^{n+1}\|_{L^2}^2, \\ 2 \Delta t b(\tilde{\mathbf{u}}_h^{n+1}, \boldsymbol{\eta}_{\mathbf{u}}^{n+1}, \boldsymbol{\Lambda}_{\mathbf{u},h}^{n+1}) &\leq 2 C \Delta t \|\nabla \tilde{\mathbf{u}}_h^{n+1}\|_{L^2} \|\nabla \boldsymbol{\eta}_{\mathbf{u}}^{n+1}\|_{L^2} \|\nabla \boldsymbol{\Lambda}_{\mathbf{u},h}^{n+1}\|_{L^2} \\ &\leq \frac{C \Delta t}{\varepsilon_7} \|\nabla \tilde{\mathbf{u}}_h^{n+1}\|_{L^2}^2 \|\nabla \boldsymbol{\eta}_{\mathbf{u}}^{n+1}\|_{L^2}^2 + \varepsilon_7 \Delta t \|\nabla \boldsymbol{\Lambda}_{\mathbf{u},h}^{n+1}\|_{L^2}^2. \end{aligned}$$

To bound the last two terms, one can apply the Cauchy-Schwarz and Young's inequalities to get: for any $q_h \in Q_h$,

$$\begin{aligned} 2 \Delta t (p^{n+1} - q_h, \nabla \cdot \boldsymbol{\Lambda}_{\mathbf{u},h}^{n+1}) &\leq 2 \Delta t \|p^{n+1} - q_h\|_{L^2} \|\nabla \boldsymbol{\Lambda}_{\mathbf{u},h}^{n+1}\|_{L^2} \\ &\leq \frac{\Delta t}{\varepsilon_8} \inf_{q_h \in Q_h} \|p^{n+1} - q_h\|_{L^2}^2 + \varepsilon_8 \Delta t \|\nabla \boldsymbol{\Lambda}_{\mathbf{u},h}^{n+1}\|_{L^2}^2, \end{aligned}$$

and

$$\begin{aligned} 2 \Delta t Ri(\langle \mathbf{0}, e_\theta^n \rangle \boldsymbol{\Lambda}_{\mathbf{u},h}^{n+1}) &\leq 2 \Delta t \left(Ri(\|\boldsymbol{\eta}_\theta^n\|_{L^2} + \|\boldsymbol{\Lambda}_{\theta,h}^n\|_{L^2}) C_P \|\nabla \boldsymbol{\Lambda}_{\mathbf{u},h}^{n+1}\|_{L^2} \right) \\ &\leq \frac{2 C_P^2 Ri^2 \Delta t}{\varepsilon_9} (\|\boldsymbol{\eta}_\theta^n\|_{L^2}^2 + \|\boldsymbol{\Lambda}_{\theta,h}^n\|_{L^2}^2) + \varepsilon_9 \Delta t \|\nabla \boldsymbol{\Lambda}_{\mathbf{u},h}^{n+1}\|_{L^2}^2. \end{aligned}$$

We now bound the terms of $E_1(\mathbf{u}, \theta, \boldsymbol{\Lambda}_{\mathbf{u},h}^{n+1})$, and note that the estimation of $E_2(\mathbf{u}, \theta, \chi_h)$ proceeds in a similar way. First apply Taylor's Theorem with integral remainder term in the first argument of each term of $E_1(\mathbf{u}, \theta, \mathbf{v}_h)$. Then use Lemma 2.1, the Young's inequality for the first and second terms, and the Cauchy-Schwarz, the Poincare and the Young's inequalities for the last term which produce

$$\begin{aligned} b(\mathbf{u}^{n+1} - \mathbf{u}^n, \mathbf{u}^{n+1}, \boldsymbol{\Lambda}_{\mathbf{u},h}^{n+1}) &\leq C \Delta t^{1/2} \|\nabla \mathbf{u}_t\|_{L^2(t^n, t^{n+1}; L^2(\Omega))} \|\nabla \mathbf{u}^{n+1}\|_{L^2} \|\nabla \boldsymbol{\Lambda}_{\mathbf{u},h}^{n+1}\|_{L^2} \\ &\leq \frac{C \Delta t}{\varepsilon_1^*} \|\nabla \mathbf{u}_t\|_{L^2(t^n, t^{n+1}; L^2(\Omega))}^2 \|\nabla \mathbf{u}^{n+1}\|_{L^2}^2 + \varepsilon_1^* \|\nabla \boldsymbol{\Lambda}_{\mathbf{u},h}^{n+1}\|_{L^2}^2, \end{aligned}$$

and

$$\begin{aligned}
Ri \left(\langle 0, \theta^{n+1} - \theta^n \rangle, \Lambda_{\mathbf{u},h}^{n+1} \right) &\leq C_P Ri \|\theta^{n+1} - \theta^n\|_{L^2} \|\nabla \Lambda_{\mathbf{u},h}^{n+1}\|_{L^2} \\
&\leq \frac{C_P^2 Ri^2 \Delta t}{\varepsilon_2^*} \|\theta_t\|_{L^2(t^n, t^{n+1}; L^2(\Omega))}^2 + \varepsilon_2^* \|\nabla \Lambda_{\mathbf{u},h}^{n+1}\|_{L^2}^2, \\
\left(\mathbf{u}_t^{n+1} - \frac{\mathbf{u}^{n+1} - \mathbf{u}^n}{\Delta t}, \Lambda_{\mathbf{u},h}^{n+1} \right) &\leq C_P \Delta t^{1/2} \|\mathbf{u}_{tt}\|_{L^2(t^n, t^{n+1}; L^2(\Omega))} \|\nabla \Lambda_{\mathbf{u},h}^{n+1}\|_{L^2} \\
&\leq \frac{C_P^2 \Delta t}{\varepsilon_3^*} \|\mathbf{u}_{tt}\|_{L^2(t^n, t^{n+1}; L^2(\Omega))}^2 + \varepsilon_3^* \|\nabla \Lambda_{\mathbf{u},h}^{n+1}\|_{L^2}^2.
\end{aligned}$$

Inserting these estimates gives

$$\begin{aligned}
E_1(\mathbf{u}, \theta, \Lambda_{\mathbf{u},h}^{n+1}) &\leq C_P^2 \Delta t \left(\frac{Ri^2}{\varepsilon_2^*} \|\theta_t\|_{L^2}^2 + \frac{1}{\varepsilon_3^*} \|\mathbf{u}_{tt}\|_{L^2(t^n, t^{n+1}; L^2(\Omega))}^2 \right) + C \Delta t \frac{1}{\varepsilon_1^*} \|\nabla \mathbf{u}^{n+1}\|_{L^2}^2 \|\nabla \mathbf{u}_t\|_{L^2(t^n, t^{n+1}; L^2(\Omega))}^2 \\
&\quad + (\varepsilon_1^* + \varepsilon_2^* + \varepsilon_3^*) \|\nabla \Lambda_{\mathbf{u},h}^{n+1}\|_{L^2}^2.
\end{aligned}$$

Step 3: The application of the Gronwall Lemma

Insert these estimates, and use Lemma 3.3. Choosing appropriate values of $\varepsilon_i, i = 1, \dots, 13$, and $\varepsilon_i^*, i = 1, \dots, 6$, produces

$$\begin{aligned}
&\|\phi_{\mathbf{u},h}^{n+1}\|_{L^2}^2 - \|\phi_{\mathbf{u},h}^n\|_{L^2}^2 + \beta \left(\|\nabla \cdot \phi_{\mathbf{u},h}^{n+1}\|_{L^2}^2 - \|\nabla \cdot \phi_{\mathbf{u},h}^n\|_{L^2}^2 \right) + \|\Lambda_{\mathbf{u},h}^{n+1} - \phi_{\mathbf{u},h}^{n+1}\|_{L^2}^2 + \|\Lambda_{\mathbf{u},h}^n - \phi_{\mathbf{u},h}^n\|_{L^2}^2 \\
&\quad + \frac{\beta}{2} \|\nabla \cdot (\phi_{\mathbf{u},h}^{n+1} - \phi_{\mathbf{u},h}^n)\|_{L^2}^2 + \gamma \Delta t \|\nabla \cdot \phi_{\mathbf{u},h}^{n+1}\|_{L^2}^2 + \nu \Delta t \|\nabla \Lambda_{\mathbf{u},h}^{n+1}\|_{L^2}^2 \\
&\leq C \nu^{-1} \|\boldsymbol{\eta}_{\mathbf{u},t}\|_{L^2(t^n, t^{n+1}; H^{-1}(\Omega))}^2 + \Delta t (C\nu + \gamma) \|\nabla \boldsymbol{\eta}_{\mathbf{u}}^{n+1}\|_{L^2}^2 + C \nu^{-1} \Delta t \|\nabla \mathbf{u}^{n+1}\|_{L^2}^2 \|\boldsymbol{\eta}_{\mathbf{u}}^n\|_{L^2} \|\nabla \boldsymbol{\eta}_{\mathbf{u}}^n\|_{L^2} \\
&\quad + C \nu^{-1} \Delta t \|\nabla \mathbf{u}^{n+1}\|_{L^3}^2 \|\phi_{\mathbf{u},h}^n\|_{L^2}^2 + \beta \Delta t \left(C \nu^{-1} \beta^{-1} \|\mathbf{u}^{n+1}\|_{L^\infty}^2 + 1 \right) \|\nabla \cdot \phi_{\mathbf{u},h}^n\|_{L^2}^2 \\
&+ C \nu^{-1} h^{-1} \Delta t \|\mathbf{u}_h^n - \tilde{\mathbf{u}}_h^{n+1}\|_{L^2}^2 \|\nabla \boldsymbol{\eta}_{\mathbf{u}}^{n+1}\|_{L^2}^2 + C \nu^{-1} \Delta t \|\nabla \tilde{\mathbf{u}}_h^{n+1}\|_{L^2}^2 \|\nabla \boldsymbol{\eta}_{\mathbf{u}}^{n+1}\|_{L^2}^2 + C \nu^{-1} \Delta t \inf_{q_h \in Q_h} \|p^{n+1} - q_h\|_{L^2}^2 \\
&\quad + C \nu^{-1} \Delta t (\|\boldsymbol{\eta}_\theta^n\|_{L^2}^2 + \|\Lambda_{\theta,h}^n\|_{L^2}^2) + \beta (1 + 2 \Delta t) \|\nabla \boldsymbol{\eta}_{\mathbf{u},t}\|_{L^2(t^n, t^{n+1}; L^2(\Omega))}^2 \\
&+ C \nu^{-1} \Delta t^2 \left(\|\mathbf{u}_{tt}\|_{L^2(t^n, t^{n+1}; L^2(\Omega))}^2 + \|\theta_t\|_{L^2(t^n, t^{n+1}; L^2(\Omega))}^2 + \|\nabla \mathbf{u}^{n+1}\|_{L^2}^2 \|\nabla \mathbf{u}_t\|_{L^2(t^n, t^{n+1}; L^2(\Omega))}^2 \right). \quad (3.20)
\end{aligned}$$

Applying similar ideas to 3.19

$$\begin{aligned}
&\|\Lambda_{\theta,h}^{n+1}\|_{L^2}^2 - \|\Lambda_{\theta,h}^n\|_{L^2}^2 + \|\Lambda_{\theta,h}^{n+1} - \Lambda_{\theta,h}^n\|_{L^2}^2 + 2 \kappa \Delta t \|\nabla \Lambda_{\theta,h}^{n+1}\|_{L^2}^2 \\
&\leq C \kappa \Delta t \|\nabla \boldsymbol{\eta}_{\mathbf{u}}^{n+1}\|_{L^2}^2 + C \kappa^{-1} \Delta t \left(\|\boldsymbol{\eta}_{\theta,t}\|_{L^2(t^n, t^{n+1}; H^{-1}(\Omega))}^2 + \|\nabla \theta^{n+1}\|_{L^2}^2 \|\boldsymbol{\eta}_{\mathbf{u}}^n\|_{L^2} \|\nabla \boldsymbol{\eta}_{\mathbf{u}}^n\|_{L^2} \right. \\
&\quad \left. + (\|\nabla \theta^{n+1}\|_{L^3}^2 + \|\theta^{n+1}\|_{L^\infty}^2) \|\phi_{\mathbf{u},h}^n\|_{L^2}^2 + h^{-1} \|\mathbf{u}_h^n - \tilde{\mathbf{u}}_h^{n+1}\|_{L^2}^2 \|\nabla \boldsymbol{\eta}_\theta^{n+1}\|_{L^2}^2 + \|\nabla \tilde{\mathbf{u}}_h^{n+1}\|_{L^2}^2 \|\nabla \boldsymbol{\eta}_\theta^{n+1}\|_{L^2}^2 \right) \\
&\quad + C \kappa^{-1} \Delta t^2 \left(\|\theta_{tt}\|_{L^2(t^n, t^{n+1}; L^2(\Omega))}^2 + \|\nabla \mathbf{u}^{n+1}\|_{L^2}^2 \|\nabla \mathbf{u}_t\|_{L^2(t^n, t^{n+1}; L^2(\Omega))}^2 \right). \quad (3.21)
\end{aligned}$$

Drop the non-negative the fourth, fifth, sixth left hand side terms of (3.20) and (3.21), use the regularity

assumptions on Boussinesq solution, and sum over time steps. This produces

$$\begin{aligned}
& \|\phi_{\mathbf{u},h}^N\|_{L^2}^2 + \beta \|\nabla \cdot \phi_{\mathbf{u},h}^N\|_{L^2}^2 + \Delta t \sum_{n=0}^{N-1} \left(\gamma \|\nabla \cdot \phi_{\mathbf{u},h}^{n+1}\|_{L^2}^2 + \nu \|\nabla \Lambda_{\mathbf{u},h}^{n+1}\|_{L^2}^2 \right) \\
& \leq \Delta t \sum_{n=0}^{N-1} \left[C \nu^{-1} \|\nabla \mathbf{u}^{n+1}\|_{L^3}^2 \|\phi_{\mathbf{u},h}^n\|_{L^2}^2 + \beta \left(\nu^{-1} \beta^{-1} \|\mathbf{u}^{n+1}\|_{L^\infty}^2 + 1 \right) \|\nabla \cdot \phi_{\mathbf{u},h}^n\|_{L^2}^2 \right. \\
& \quad \left. + \kappa^{-1} \left(\|\nabla \theta^{n+1}\|_{L^3}^2 + \|\theta^{n+1}\|_{L^\infty}^2 \right) \|\phi_{\mathbf{u},h}^n\|_{L^2}^2 \right] \\
& + \Delta t \sum_{n=0}^{N-1} C \nu^{-1} \left(h^{-1} \|\mathbf{u}_h^n - \tilde{\mathbf{u}}_h^{n+1}\|_{L^2}^2 \|\nabla \boldsymbol{\eta}_{\mathbf{u}}^{n+1}\|_{L^2}^2 + \|\nabla \tilde{\mathbf{u}}_h^{n+1}\|_{L^2}^2 \|\nabla \boldsymbol{\eta}_{\mathbf{u}}^{n+1}\|_{L^2}^2 \right) + \|\phi_{\mathbf{u},h}^0\|_{L^2}^2 + \beta \|\nabla \cdot \phi_{\mathbf{u},h}^0\|_{L^2}^2 \\
& + C \left[\nu^{-1} h^{2k+2} + (\nu + \gamma) h^{2k} + \nu^{-1} h^{2k} + \beta (1 + 2 \Delta t) h^{2k} + \nu^{-1} \Delta t^2 \right], \tag{3.22}
\end{aligned}$$

and

$$\begin{aligned}
& \|\Lambda_{\theta,h}^N\|_{L^2}^2 + \kappa \Delta t \sum_{n=0}^{N-1} \|\nabla \Lambda_{\theta,h}^{n+1}\|_{L^2}^2 \leq \Delta t \sum_{n=0}^{N-1} \kappa^{-1} \left(\|\nabla \theta^{n+1}\|_{L^3}^2 + \|\theta^{n+1}\|_{L^\infty}^2 \right) \|\phi_{\mathbf{u},h}^n\|_{L^2}^2 \\
& + \Delta t \sum_{n=0}^{N-1} C \kappa^{-1} \left(\|\nabla \theta^{n+1}\|_{L^2}^2 \|\boldsymbol{\eta}_{\mathbf{u}}^n\|_{L^2}^2 \|\nabla \boldsymbol{\eta}_{\mathbf{u}}^n\|_{L^2}^2 + h^{-1} \|\mathbf{u}_h^n - \tilde{\mathbf{u}}_h^{n+1}\|_{L^2}^2 \|\nabla \boldsymbol{\eta}_{\theta}^{n+1}\|_{L^2}^2 + \|\nabla \tilde{\mathbf{u}}_h^{n+1}\|_{L^2}^2 \|\nabla \boldsymbol{\eta}_{\theta}^{n+1}\|_{L^2}^2 \right) \\
& + C \kappa^{-1} \left(h^{2k+2} + \Delta t h^{2k-1} + h^{2k} + \Delta t^2 \right) + \|\Lambda_{\theta,h}^0\|_{L^2}^2. \tag{3.23}
\end{aligned}$$

Add (3.23) to (3.22), and notice that $\phi_{\mathbf{u},h}^0 = 0$, $\Lambda_{\theta,h}^0 = 0$. Then apply discrete Gronwall Lemma which yields:

$$\begin{aligned}
& \|\phi_{\mathbf{u},h}^N\|_{L^2}^2 + \beta \|\nabla \cdot \phi_{\mathbf{u},h}^N\|_{L^2}^2 + \|\Lambda_{\theta,h}^N\|_{L^2}^2 + \gamma \|\nabla \cdot \phi_{\mathbf{u},h}\|_{2,0}^2 + \nu \|\nabla \Lambda_{\mathbf{u},h}\|_{2,0}^2 + \kappa \|\nabla \Lambda_{\theta,h}\|_{2,0}^2 \\
& \leq C \left[(\nu^{-1} + \kappa^{-1}) h^{2k+2} + (\nu + \gamma + \kappa) h^{2k} + (\nu^{-1} + \kappa^{-1}) \Delta t h^{2k-1} + \beta (1 + 2 \Delta t) h^{2k} + (\nu^{-1} + \kappa^{-1}) \Delta t^2 \right]. \tag{3.24}
\end{aligned}$$

Step 4: The completion of the proof

The application of the triangle inequality to all error terms gives

$$\begin{aligned}
& \|e_{\mathbf{u}}^N\|_{L^2}^2 + \|e_{\theta}^N\|_{L^2}^2 + \beta \|\nabla \cdot \mathbf{e}_{\mathbf{u}}^N\|_{L^2}^2 + \gamma \|\nabla \cdot \mathbf{e}_{\mathbf{u}}\|_{2,0}^2 + \nu \|\nabla \mathbf{e}_{\mathbf{u}}\|_{2,0}^2 + \kappa \|\nabla e_{\theta}\|_{2,0}^2 \\
& \leq 2 \left(\|\boldsymbol{\eta}_{\mathbf{u}}^N\|_{L^2}^2 + \|\boldsymbol{\eta}_{\theta}^N\|_{L^2}^2 + \beta \|\nabla \cdot \boldsymbol{\eta}_{\mathbf{u}}^N\|_{L^2}^2 + \gamma \|\nabla \cdot \boldsymbol{\eta}_{\mathbf{u}}\|_{2,0}^2 + \nu \|\nabla \boldsymbol{\eta}_{\mathbf{u}}\|_{2,0}^2 + \kappa \|\nabla \boldsymbol{\eta}_{\theta}\|_{2,0}^2 \right) \\
& + 2 \left(\|\phi_{\mathbf{u},h}^N\|_{L^2}^2 + \|\Lambda_{\theta,h}^N\|_{L^2}^2 + \beta \|\nabla \cdot \phi_{\mathbf{u},h}^N\|_{L^2}^2 + \gamma \|\nabla \cdot \phi_{\mathbf{u},h}\|_{2,0}^2 + \nu \|\nabla \Lambda_{\mathbf{u},h}\|_{2,0}^2 + \kappa \|\nabla \Lambda_{\theta,h}\|_{2,0}^2 \right).
\end{aligned}$$

Finally, using the regularity assumptions on the Boussinesq solutions, approximation properties, and estimate (3.24) finishes the proof. \square

Numerical Experiments

This section presents two numerical experiments to test the predicted convergence rates of the previous section, and illustrate the reliability of Algorithm 3.1. All tests are implemented using FreeFem++ [20].

3.2.1 Convergence Rate Verification

With the use of the finite element spaces (\mathbf{P}_2, P_1, P_2) for the velocity/pressure/temperature, respectively, Theorem 3.1 concludes the second order convergence in space provided $\Delta t \leq h$. To verify that, we choose a test problem which has solution

$$\mathbf{u}(\mathbf{x}, t) := \langle e^t \cos(\pi(y - t)), e^t \sin(\pi(x + t)) \rangle, \quad p(\mathbf{x}, t) := \sin(x + y)(1 + t^2),$$

on the unit square $(0, 1)^2$ with $\nu = 1$, $Ri = 1$, $\kappa = 1$, and stabilization parameters $\gamma = 1.0$ and $\beta = 1.0$. The forcing terms \mathbf{f}, Ψ are calculated from \mathbf{u}, p, θ and the Boussinesq equations. Then, we compute solutions to Algorithm 3.1 on a series of refined mesh by choosing an end time $T = 0.001$ and time step $\Delta t = 0.0001$. The results are presented in Table 1, and are consistent with our theoretical findings for convergence rates. We next test the predicted temporal rates using the same test problem. We run our method on a fixed mesh with mesh size $h = 1/64$ with a series of timesteps. The computed errors and rates are presented in Table 2. Again we observe the predicted optimal rates. Note that the divergence error is always small here, due to the finer mesh and the stabilization. Since this error is already as small as linear solver error, we do not expect convergence rates (as it has already converged).

Table 1: Spatial velocity errors and rates for a fixed end time $T = 0.001$, a time step $\Delta t = 0.0001$.

h	$\ \mathbf{u} - \mathbf{u}_h\ _{\infty,0}$	Rate	$\ \nabla \cdot (\mathbf{u} - \mathbf{u}_h)\ _{\infty,0}$	Rate	$\ \nabla \cdot (\mathbf{u} - \mathbf{u}_h)\ _{2,0}$	Rate	$\ \nabla(\mathbf{u} - \tilde{\mathbf{u}}_h)\ _{2,0}$	Rate
1/4	$1.9978e-2$	—	$1.9001e-5$	—	$1.1808e-7$	—	$2.7976e-3$	—
1/8	$2.5644e-3$	2.9618	$5.5915e-6$	1.7648	$3.4854e-8$	1.7604	$7.1600e-4$	1.9662
1/16	$3.2267e-4$	2.9904	$1.2480e-6$	2.1636	$7.7778e-9$	2.1639	$1.7974e-4$	1.9940
1/32	$4.0400e-5$	2.9976	$2.8658e-7$	2.1226	$1.7864e-9$	2.1222	$4.4702e-5$	2.0075
1/64	$5.0521e-6$	2.9994	$6.0716e-8$	2.2388	$3.8071e-10$	2.2388	$1.0964e-5$	2.0274

Table 2: Temporal velocity errors and rates on a fixed mesh size $h = 1/64$.

Δt	$\ \mathbf{u} - \mathbf{u}_h\ _{\infty,0}$	Rate	$\ \nabla \cdot (\mathbf{u} - \mathbf{u}_h)\ _{\infty,0}$	Rate	$\ \nabla \cdot (\mathbf{u} - \mathbf{u}_h)\ _{2,0}$	Rate	$\ \nabla(\mathbf{u} - \tilde{\mathbf{u}}_h)\ _{2,0}$	Rate
1/4	$4.1914e-2$	—	$3.3464e-8$	—	$2.1720e-8$	—	$2.4817e-1$	—
1/8	$2.7726e-2$	0.5962	$3.6204e-8$	—	$2.1113e-8$	—	$1.4157e-1$	0.8098
1/16	$1.5418e-2$	0.8467	$4.3557e-8$	—	$2.5392e-8$	—	$7.3314e-2$	0.9494
1/32	$8.0705e-3$	0.9339	$6.3380e-8$	—	$3.8401e-8$	—	$3.7046e-2$	0.9848
1/64	$4.1217e-3$	0.9694	$1.0736e-8$	—	$6.4309e-8$	—	$1.8595e-2$	0.9944

3.2.2 Marsigli Experiment

This numerical experiment tests the proposed algorithm and reveals its effectiveness on a physical situation, which was described by Marsigli in 1681. This physical situation demonstrates that when two fluids with different densities meet, a motion driven by the gravitational force is created: the fluid with higher density rises over the lower one. Since the density differences can be modelled by the temperature differences with the help of the Boussinesq approximation, this physical problem is modelled by the incompressible Boussinesq system (3.1) studied herein.

In the problem set-up, we follow the paper [33] of H. Johnston et al. The flow region taken is an insulated box $[0, 8] \times [0, 1]$ divided at $x = 4$. The initial velocity is taken to be zero since the flow is at rest, and the initial temperature on the left hand side of the box is $\theta_0 = 1.5$, and on the right hand side $\theta_0 = 1.0$. The dimensionless flow parameters are set to be $Re = 1,000$, $Ri = 4$, $Pr = 1$, and the flow starts from rest.

The first results we present are the direct numerical simulations (DNS) of the Boussinesq equations. We use finite element spaces (\mathbf{P}_2, P_1, P_2) for the velocity/pressure/temperature, respectively, on a finer, unstructured mesh, which provides 135,642 velocity dof, 17,111 pressure dof and 67,821 temperature dof. All solutions are computed at $T = 2, 4, 8$, taking a time step $\Delta t = 0.025$. Our goal is to compare our scheme with the BE-FE method (i.e. no stabilization), and standard grad-div method with stabilization parameter 1.0 on this physical problem on coarser meshes then is required by a DNS. In order to realize this aim, these three schemes

are solved on the same moderately fine mesh, which gives 26,082 velocity dof, 3,321 pressure dof and 13,041 temperature dof. We imposed homogeneous Dirichlet boundary conditions for the velocity and the adiabatic boundary condition for the temperature, and used (\mathbf{P}_2, P_1, P_2) for the velocity/pressure/temperature finite element spaces, respectively. All solutions are calculated at $T = 2, 4, 8$ taking a time step $\Delta t = 0.025$ with the same flow parameters as the DNS. The results are presented in Figures 2, 3 and 4. It can be clearly seen that the modular grad-div method catches very well the flow pattern and temperature distribution of the DNS at each time level. Also it gives very similar results to the standard grad-div method (with parameter 1.0) at each time level. However, the non-stabilized solution creates very poor solutions, and significant oscillations build in temperature and velocity as time progresses.

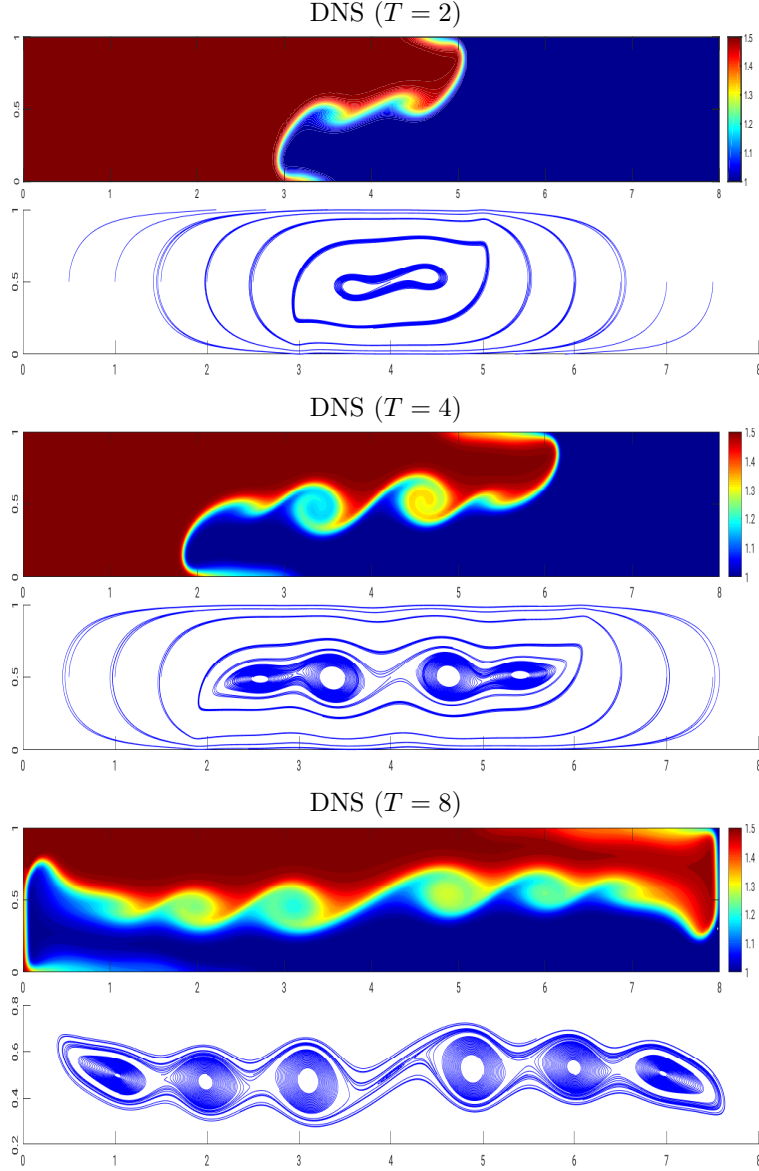


Figure 1: The resolved temperature contours and velocity streamlines, from a fine mesh computation at end times $T = 2, 4, 8$ with $\Delta t = 0.025$, $Re = 1,000$, $Pr = 1$, and $Ri = 4$.

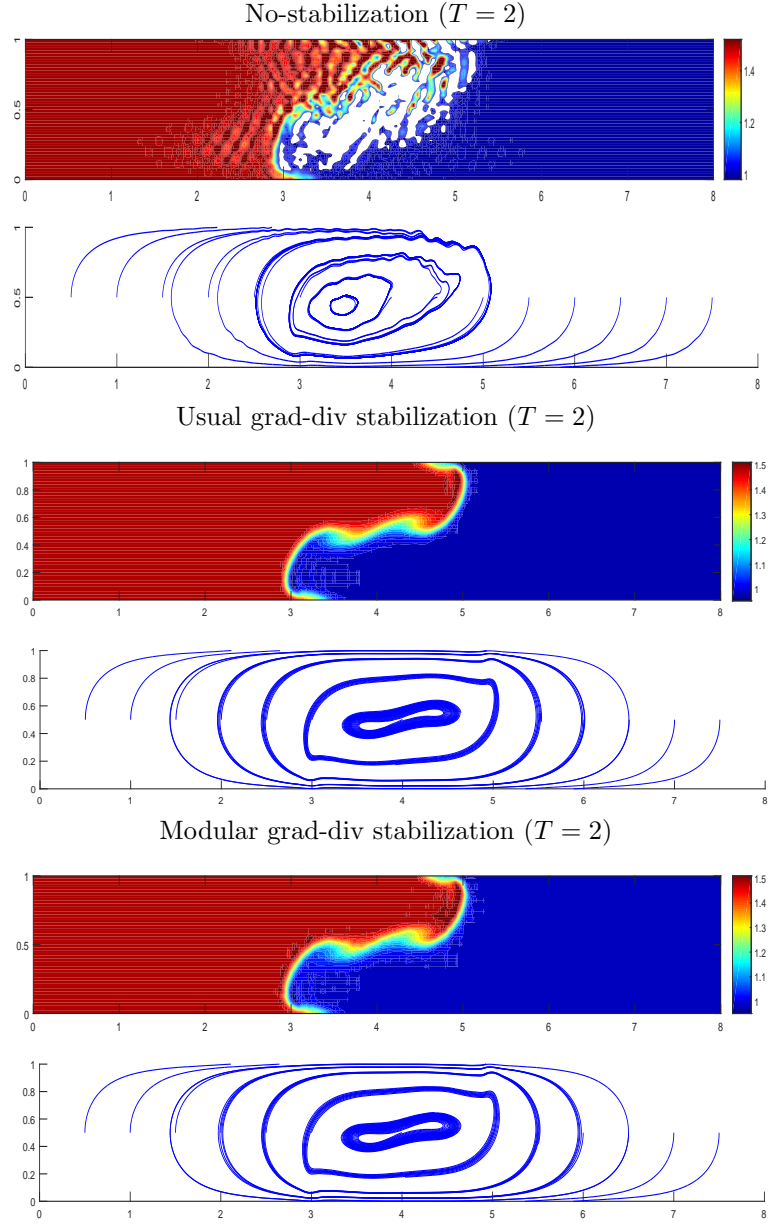


Figure 2: The temperature contours and velocity streamlines of BE-FEM (no-stabilization), the usual grad-div, and the modular grad-div, respectively, from a coarse mesh computation at $T = 2$ with $\Delta t = 0.025$, $Re = 1,000$, $Pr = 1$, and $Ri = 4$.

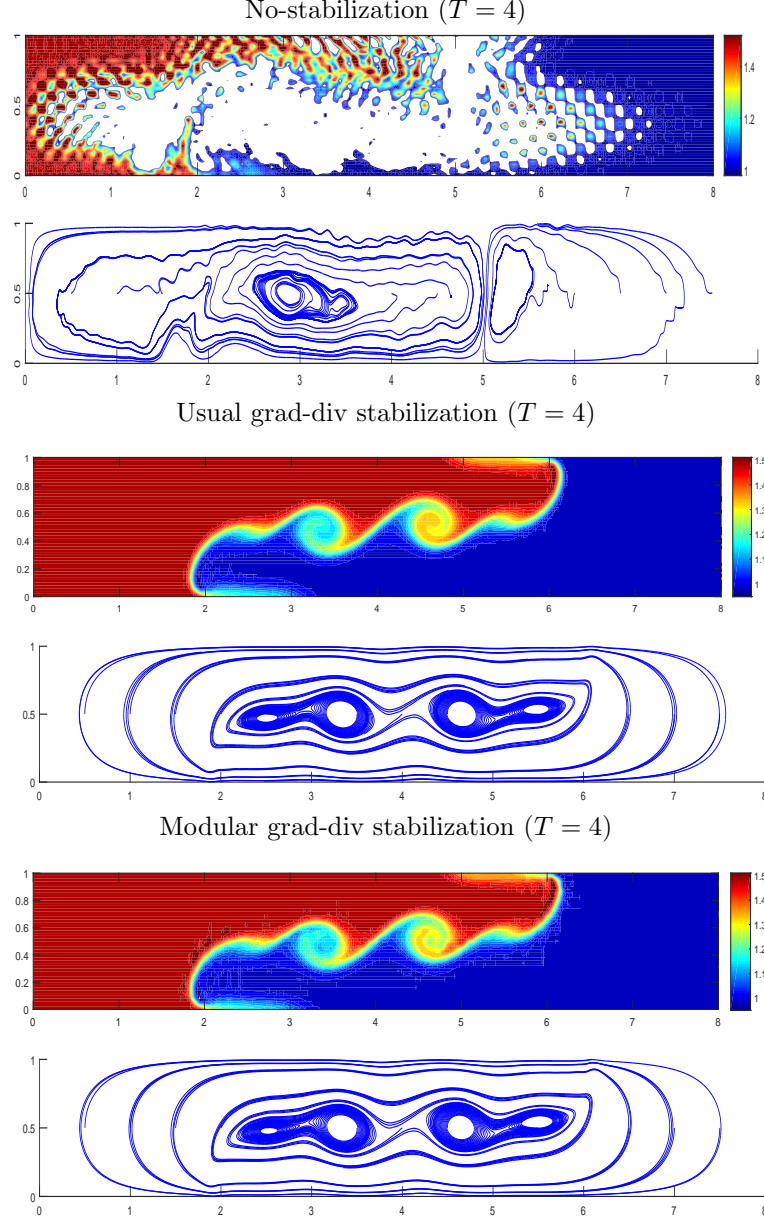


Figure 3: The temperature contours and velocity streamlines of BE-FEM (no-stabilization), the usual grad-div, and the modular grad-div, respectively, from a coarse mesh computation at $T = 4$ with $\Delta t = 0.025$, $Re = 1,000$, $Pr = 1$, and $Ri = 4$.

4 **Second order** modular grad-div stabilization for MHD equations

This section considers **second order** modular grad-div stabilization applied to magnetohydrodynamic (MHD) flows discretizations. The governing system of evolution equations we consider is [26, 3]:

$$\begin{aligned}
 \mathbf{u}_t - \nu \Delta \mathbf{u} + (\mathbf{u} \cdot \nabla) \mathbf{u} - s(\mathbf{B} \cdot \nabla) \mathbf{B} + \nabla P &= \mathbf{f}, \\
 \nabla \cdot \mathbf{u} &= 0, \\
 \mathbf{B}_t - \nu_m \Delta \mathbf{B} + (\mathbf{u} \cdot \nabla) \mathbf{B} - (\mathbf{B} \cdot \nabla) \mathbf{u} - \nabla \lambda &= \nabla \times \mathbf{g}, \\
 \nabla \cdot \mathbf{B} &= 0,
 \end{aligned} \tag{4.1}$$

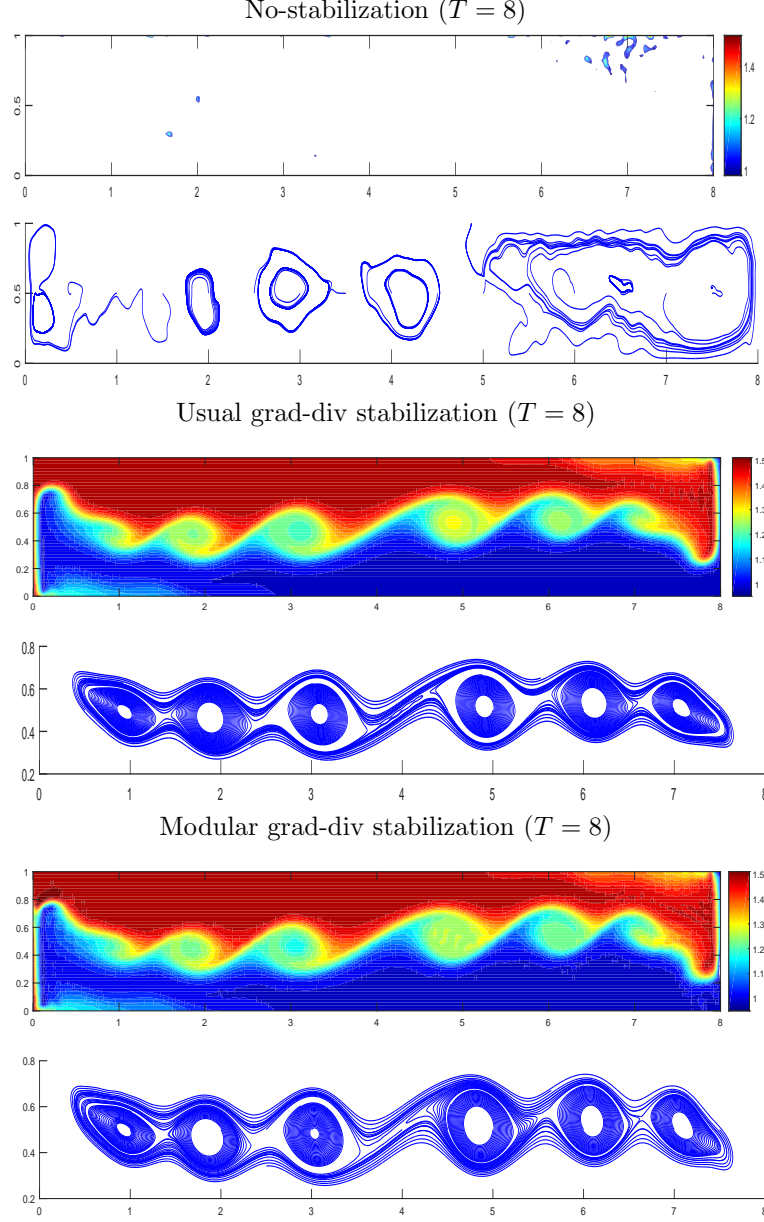


Figure 4: The temperature contours and velocity streamlines of BE-FEM (no-stabilization), the usual grad-div, and the modular grad-div, respectively, from a coarse mesh computation at $T = 8$ with $\Delta t = 0.025$, $Re = 1,000$, $Pr = 1$, and $Ri = 4$.

in $\Omega \times (0, T)$, where Ω is the domain of the fluid, $\mathbf{u} := (u_1(\mathbf{x}, t), u_2(\mathbf{x}, t), u_3(\mathbf{x}, t))$ is the velocity of the fluid, $P := p(\mathbf{x}, t) + \frac{1}{2}|u(t^n)|^2$ is the Bernoulli pressure where $p(\mathbf{x}, t)$ is the pressure, $\mathbf{B} := (B_1(\mathbf{x}, t), B_2(\mathbf{x}, t), B_3(\mathbf{x}, t))$ is the magnetic field, and λ is a Lagrange multiplier corresponding to the solenoidal constraint on the magnetic field. Moreover, ν is the kinematic viscosity, s is the coupling number and ν_m is the magnetic resistivity, \mathbf{f} is the body force, and $\nabla \times \mathbf{g}$ is the forcing on the magnetic field. The physical principles governing such flows are that when an electrically conducting fluid moves in a magnetic field, the magnetic field induces currents in the fluid, which in turn creates forces on the fluid and also changes the magnetic field. In recent

years, the study of MHD flows has become important due to applications in, e.g. astrophysics and geophysics [22, 41, 13, 10, 9, 2, 4, 39], liquid metal cooling of nuclear reactors [1, 19, 43], and process metallurgy [8].

We note that the first order modular grad-div method (MGD) with backward-Euler time discretization for MHD was considered in [34], where MHD equations are expressed with different formulations. In that paper, the authors provide the stability and convergence analysis of the algorithm, and test it on a classical benchmark problem, Hartmann flow. We improve on these results herein in two ways, first by considering the second order modular grad-div step with linearly extrapolated BDF2 method for approximating the MHD model. Second, since one advantage of the classical grad-div stabilization is to reduce the negative effect of the pressure on the velocity error, we focus on our numerical experiments whether the MGD method has similar effect or not, which is not considered in the recent paper [34]. Our experiments reveal that the modular grad-div stabilization penalizes the divergence stronger than the usual grad-div-stabilization.

The proposed algorithm consists of two decoupled steps at each time level as in the Boussinesq case. The first step approximates the MHD equations using **BDF2LE temporal**, and finite element spatial discretization. The second step consists of two **second order** modular grad-div stabilizations: one is for the velocity, and the other for the magnetic field. The algorithm is given below:

Algorithm 4.1. *Let forcing terms \mathbf{f} , $\nabla \times \mathbf{g}$ and initial conditions \mathbf{u}_h^0 , \mathbf{B}_h^0 be given. Choose an end time T and a time step Δt such that $T = N \Delta t$. Denote the discrete solutions at time levels $t^n := n \Delta t$, $n = 0, 1, 2, \dots, N$, by*

$$\mathbf{u}_h^n := \mathbf{u}_h(t^n), \quad \mathbf{B}_h^n := \mathbf{B}_h(t^n), \quad p_h^n := p_h(t^n), \quad \lambda_h^n := \lambda_h(t^n).$$

For all $n = 0, 1, \dots, N - 1$, find $(\mathbf{u}_h^{n+1}, p_h^{n+1}, \mathbf{B}_h^{n+1}, \lambda_h^{n+1})$ via the following two steps:

Step 1: *Given $(\mathbf{u}_h^n, \mathbf{B}_h^n) \in \mathbf{X}_h \times \mathbf{X}_h$, find $(\tilde{\mathbf{u}}_h^{n+1}, p_h^{n+1}, \tilde{\mathbf{B}}_h^{n+1}, \lambda_h^{n+1}) \in \mathbf{X}_h \times Q_h \times \mathbf{X}_h \times Q_h$ such that for all $(\mathbf{v}_h, q_h, \mathbf{w}_h, r_h) \in \mathbf{X}_h \times Q_h \times \mathbf{X}_h \times Q_h$ it holds*

$$\left(\frac{3\tilde{\mathbf{u}}_h^{n+1} - 4\mathbf{u}_h^n + \mathbf{u}_h^{n-1}}{2\Delta t}, \mathbf{v}_h \right) + \nu(\nabla \tilde{\mathbf{u}}_h^{n+1}, \nabla \mathbf{v}_h) + b(2\mathbf{u}_h^n - \mathbf{u}_h^{n-1}, \tilde{\mathbf{u}}_h^{n+1}, \mathbf{v}_h) \quad (4.2)$$

$$\begin{aligned} -sb(2\mathbf{B}_h^n - \mathbf{B}_h^{n-1}, \tilde{\mathbf{B}}_h^{n+1}, \mathbf{v}_h) - (p_h^{n+1}, \nabla \cdot \mathbf{v}_h) &= (\mathbf{f}^{n+1}, \mathbf{v}_h), \\ (\nabla \cdot \tilde{\mathbf{u}}_h^{n+1}, q_h) &= 0, \end{aligned} \quad (4.3)$$

$$\left(\frac{3\tilde{\mathbf{B}}_h^{n+1} - 4\mathbf{B}_h^n + \mathbf{B}_h^{n-1}}{2\Delta t}, \mathbf{w}_h \right) + \nu_m(\nabla \tilde{\mathbf{B}}_h^{n+1}, \nabla \mathbf{w}_h) + b(2\mathbf{u}_h^n - \mathbf{u}_h^{n-1}, \tilde{\mathbf{B}}_h^{n+1}, \mathbf{w}_h) \quad (4.4)$$

$$\begin{aligned} -b(2\mathbf{B}_h^n - \mathbf{u}_h^{n-1}, \tilde{\mathbf{u}}_h^{n+1}, \mathbf{w}_h) + (\lambda_h^{n+1}, \nabla \cdot \mathbf{w}_h) &= (\nabla \times \mathbf{g}^{n+1}, \mathbf{w}_h), \\ (\nabla \cdot \tilde{\mathbf{B}}_h^{n+1}, r_h) &= 0. \end{aligned} \quad (4.5)$$

Step 2: *For $(\tilde{\mathbf{u}}_h^{n+1}, \tilde{\mathbf{B}}_h^{n+1}) \in \mathbf{X}_h \times \mathbf{X}_h$, find $(\mathbf{u}_h^{n+1}, \mathbf{B}_h^{n+1}) \in \mathbf{X}_h \times \mathbf{X}_h$ such that for all $(\mathbf{v}_h, \mathbf{w}_h) \in \mathbf{X}_h \times \mathbf{X}_h$ it holds*

$$\left(\frac{3\mathbf{u}_h^{n+1} - 3\tilde{\mathbf{u}}_h^{n+1}}{2\Delta t}, \mathbf{v}_h \right) + \beta \left(\nabla \cdot \frac{3\mathbf{u}_h^{n+1} - 4\mathbf{u}_h^n + \mathbf{u}_h^{n-1}}{2\Delta t}, \nabla \cdot \mathbf{v}_h \right) + \gamma(\nabla \cdot \mathbf{u}_h^{n+1}, \nabla \cdot \mathbf{v}_h) = 0, \quad (4.6)$$

$$\left(\frac{3\mathbf{B}_h^{n+1} - 3\tilde{\mathbf{B}}_h^{n+1}}{2\Delta t}, \mathbf{w}_h \right) + \beta \left(\nabla \cdot \frac{3\mathbf{B}_h^{n+1} - 4\mathbf{B}_h^n + \mathbf{B}_h^{n-1}}{2\Delta t}, \nabla \cdot \mathbf{w}_h \right) + \gamma(\nabla \cdot \mathbf{B}_h^{n+1}, \nabla \cdot \mathbf{w}_h) = 0. \quad (4.7)$$

4.1 Stability and Convergence Results

We first prove that the method's solutions are unconditionally stable with respect to time. In the proof, we need the following two lemmas.

Lemma 4.1. *Consider the second step of Algorithm 4.1. Then it holds*

$$\begin{aligned}
& 3(\|\tilde{\mathbf{u}}_h^{n+1}\|^2 - \|\mathbf{u}_h^{n+1}\|^2 - \|\tilde{\mathbf{u}}_h^{n+1} - \mathbf{u}_h^{n+1}\|^2) \\
& = \beta (\|\nabla \cdot \mathbf{u}_h^{n+1}\|^2 - \|\nabla \cdot \mathbf{u}_h^n\|^2 + \|\nabla \cdot (2\mathbf{u}_h^{n+1} - \mathbf{u}_h^n)\|^2 - \|\nabla \cdot (2\mathbf{u}_h^n - \mathbf{u}_h^{n-1})\|^2) \\
& \quad + \beta \|\nabla \cdot (\mathbf{u}_h^{n+1} - 2\mathbf{u}_h^n + \mathbf{u}_h^{n-1})\|^2 + 4\gamma\Delta t \|\nabla \cdot \mathbf{u}_h^{n+1}\|^2, \\
& 3(\|\tilde{\mathbf{B}}_h^{n+1}\|^2 - \|\mathbf{B}_h^{n+1}\|^2 - \|\tilde{\mathbf{B}}_h^{n+1} - \mathbf{B}_h^{n+1}\|^2) \\
& = \beta (\|\nabla \cdot \mathbf{B}_h^{n+1}\|^2 - \|\nabla \cdot \mathbf{B}_h^n\|^2 + \|\nabla \cdot (2\mathbf{B}_h^{n+1} - \mathbf{B}_h^n)\|^2 - \|\nabla \cdot (2\mathbf{B}_h^n - \mathbf{B}_h^{n-1})\|^2) \\
& \quad + \beta \|\nabla \cdot (\mathbf{B}_h^{n+1} - 2\mathbf{B}_h^n + \mathbf{B}_h^{n-1})\|^2 + 4\gamma\Delta t \|\nabla \cdot \mathbf{B}_h^{n+1}\|^2.
\end{aligned}$$

Proof. Choose $\mathbf{v}_h = 4\Delta t \mathbf{u}_h^{n+1}$ in (4.6), and $\mathbf{w}_h = 4\Delta t \mathbf{B}_h^{n+1}$ in (4.7) which produces

$$6(\mathbf{u}_h^{n+1} - \tilde{\mathbf{u}}_h^{n+1}, \mathbf{u}_h^{n+1}) + 2\beta(\nabla \cdot (3\mathbf{u}_h^{n+1} - 4\mathbf{u}_h^n + \mathbf{u}_h^{n-1}), \nabla \cdot \mathbf{u}_h^{n+1}) + 4\gamma\Delta t \|\nabla \cdot \mathbf{u}_h^{n+1}\|^2 = 0, \quad (4.8)$$

$$6(\mathbf{B}_h^{n+1} - \tilde{\mathbf{B}}_h^{n+1}, \mathbf{B}_h^{n+1}) + 2\beta(\nabla \cdot (3\mathbf{B}_h^{n+1} - 4\mathbf{B}_h^n + \mathbf{B}_h^{n-1}), \nabla \cdot \mathbf{B}_h^{n+1}) + 4\gamma\Delta t \|\nabla \cdot \mathbf{B}_h^{n+1}\|^2 = 0. \quad (4.9)$$

Then using the algebraic identity $2(a - b, a) = a^2 - b^2 + (a - b)^2$ on the first terms, $4(3a - 4b + c, a) = a^2 - b^2 + (2a - b)^2 - (2b - c)^2 + (a - 2b + c)^2$ on the second terms, and rearranging finishes the proof. \square

Lemma 4.2. *Consider the second step of Algorithm 4.1. Then, it holds*

$$\begin{aligned}
(3\mathbf{u}_h^{n+1} - 4\mathbf{u}_h^n + \mathbf{u}_h^{n-1}, \tilde{\mathbf{u}}_h^{n+1} - \mathbf{u}_h^{n+1}) & = \frac{\beta}{3} \|\nabla \cdot (3\mathbf{u}_h^{n+1} - 4\mathbf{u}_h^n + \mathbf{u}_h^{n-1})\|^2 \\
& \quad + \frac{2\gamma\Delta t}{3} (\nabla \cdot \mathbf{u}_h^{n+1}, \nabla \cdot (3\mathbf{u}_h^{n+1} - 4\mathbf{u}_h^n + \mathbf{u}_h^{n-1})), \\
(3\mathbf{B}_h^{n+1} - 4\mathbf{B}_h^n + \mathbf{B}_h^{n-1}, \tilde{\mathbf{B}}_h^{n+1} - \mathbf{B}_h^{n+1}) & = \frac{\beta}{3} \|\nabla \cdot (3\mathbf{B}_h^{n+1} - 4\mathbf{B}_h^n + \mathbf{B}_h^{n-1})\|^2 \\
& \quad + \frac{2\gamma\Delta t}{3} (\nabla \cdot \mathbf{B}_h^{n+1}, \nabla \cdot (3\mathbf{B}_h^{n+1} - 4\mathbf{B}_h^n + \mathbf{B}_h^{n-1})).
\end{aligned}$$

Proof. Setting $\mathbf{v}_h = 3\mathbf{u}_h^{n+1} - 4\mathbf{u}_h^n + \mathbf{u}_h^{n-1}$ and $\mathbf{w}_h = 3\mathbf{B}_h^{n+1} - 4\mathbf{B}_h^n + \mathbf{B}_h^{n-1}$, multiplying by $2\Delta t/3$ and rearranging terms gives the desired equality. \square

Theorem 4.1. *Assume that $\mathbf{f}, \nabla \times \mathbf{g} \in L^2(0, T; \mathbf{H}^{-1}(\Omega))$. Then solutions to Algorithm 4.1 satisfy the following: for any $\Delta t > 0$*

$$\begin{aligned}
& \|\mathbf{u}_h^N\|_{L^2}^2 + \|2\mathbf{u}_h^N - \mathbf{u}_h^{N-1}\|_{L^2}^2 + s(\|\mathbf{B}_h^N\|_{L^2}^2 + \|2\mathbf{B}_h^N - \mathbf{B}_h^{N-1}\|_{L^2}^2) \\
& + \left(\beta + \frac{2\gamma\Delta t}{3}\right) \left(\|\nabla \cdot \mathbf{u}_h^N\|_{L^2}^2 + \|\nabla \cdot (2\mathbf{u}_h^N - \mathbf{u}_h^{N-1})\|_{L^2}^2 + s(\|\nabla \cdot \mathbf{B}_h^N\|_{L^2}^2 + \|\nabla \cdot (2\mathbf{B}_h^N - \mathbf{B}_h^{N-1})\|_{L^2}^2)\right) \\
& + 4\gamma\Delta t \sum_{n=0}^{N-1} \left(\|\nabla \cdot \mathbf{u}_h^{n+1}\|_{L^2}^2 + s\|\nabla \cdot \mathbf{B}_h^{n+1}\|_{L^2}^2\right) + 2\nu\Delta t \sum_{n=0}^{N-1} \|\nabla \tilde{\mathbf{u}}_h^{n+1}\|_{L^2}^2 + 2s\nu_m\Delta t \sum_{n=0}^{N-1} \|\nabla \tilde{\mathbf{B}}_h^{n+1}\|_{L^2}^2 \\
& \leq \|\mathbf{u}_h^1\|_{L^2}^2 + \|2\mathbf{u}_h^1 - \mathbf{u}_h^0\|_{L^2}^2 + s(\|\mathbf{B}_h^1\|_{L^2}^2 + \|2\mathbf{B}_h^1 - \mathbf{B}_h^0\|_{L^2}^2) \\
& \quad + \left(\beta + \frac{2\gamma\Delta t}{3}\right) \left(\|\nabla \cdot \mathbf{u}_h^1\|_{L^2}^2 + \|\nabla \cdot (2\mathbf{u}_h^1 - \mathbf{u}_h^0)\|_{L^2}^2 + s(\|\nabla \cdot \mathbf{B}_h^1\|_{L^2}^2 + \|\nabla \cdot (2\mathbf{B}_h^1 - \mathbf{B}_h^0)\|_{L^2}^2)\right) \\
& \quad + 2\nu^{-1}\Delta t \sum_{n=0}^{N-1} \|\mathbf{f}^{n+1}\|_{-1}^2 + 2s\nu_m^{-1}\Delta t \sum_{n=0}^{N-1} \|\nabla \times \mathbf{g}^{n+1}\|_{-1}^2.
\end{aligned}$$

Proof. Setting $\mathbf{v}_h = \tilde{\mathbf{u}}_h^{n+1}$ in (4.2), $q_h = P_h^{n+1}$ in (4.3), $\mathbf{w}_h = \tilde{\mathbf{B}}_h^{n+1}$ in (4.4), $r_h = \lambda_h^{n+1}$ in (4.5) and rewriting

time derivatives produces

$$\begin{aligned}
& \left(\frac{3\tilde{\mathbf{u}}_h^{n+1} - 3\mathbf{u}_h^{n+1}}{2\Delta t}, \tilde{\mathbf{u}}_h^{n+1} \right) + \left(\frac{3\mathbf{u}_h^{n+1} - 4\mathbf{u}_h^n + \mathbf{u}_h^{n-1}}{2\Delta t}, \tilde{\mathbf{u}}_h^{n+1} - \mathbf{u}_h^{n+1} \right) + \left(\frac{3\mathbf{u}_h^{n+1} - 4\mathbf{u}_h^n + \mathbf{u}_h^{n-1}}{2\Delta t}, \mathbf{u}_h^{n+1} \right) \\
& \quad + \nu \|\nabla \tilde{\mathbf{u}}_h^{n+1}\|^2 - sb(2\mathbf{B}_h^n - \mathbf{B}_h^{n-1}, \tilde{\mathbf{B}}_h^{n+1}, \tilde{\mathbf{u}}_h^{n+1}) = (\mathbf{f}^{n+1}, \tilde{\mathbf{u}}_h^{n+1}), \\
& \left(\frac{3\tilde{\mathbf{B}}_h^{n+1} - 3\mathbf{B}_h^{n+1}}{2\Delta t}, \tilde{\mathbf{B}}_h^{n+1} \right) + \left(\frac{3\mathbf{B}_h^{n+1} - 4\mathbf{B}_h^n + \mathbf{B}_h^{n-1}}{2\Delta t}, \tilde{\mathbf{B}}_h^{n+1} - \mathbf{B}_h^{n+1} \right) + \left(\frac{3\mathbf{B}_h^{n+1} - 4\mathbf{B}_h^n + \mathbf{B}_h^{n-1}}{2\Delta t}, \mathbf{B}_h^{n+1} \right) \\
& \quad + \nu_m \|\nabla \tilde{\mathbf{B}}_h^{n+1}\|^2 - b(2\mathbf{B}_h^n - \mathbf{B}_h^{n-1}, \tilde{\mathbf{u}}_h^{n+1}, \tilde{\mathbf{B}}_h^{n+1}) = (\nabla \times \mathbf{g}^{n+1}, \tilde{\mathbf{B}}_h^{n+1}).
\end{aligned}$$

First apply the Cauchy-Schwarz and the Young's inequalities to the forcing terms. Then use the algebraic identities $2(a - b, a) = a^2 - b^2 + (a - b)^2$, $4(3a - 4b + c, a) = a^2 - b^2 + (2a - b)^2 - (2b - c)^2 + (a - 2b + c)^2$ and multiply by $4\Delta t$. This yields

$$\begin{aligned}
& 3(\|\tilde{\mathbf{u}}_h^{n+1}\|^2 - \|\mathbf{u}_h^{n+1}\|^2 + \|\tilde{\mathbf{u}}_h^{n+1} - \mathbf{u}_h^{n+1}\|^2) + 2(3\mathbf{u}_h^{n+1} - 4\mathbf{u}_h^n + \mathbf{u}_h^{n-1}, \tilde{\mathbf{u}}_h^{n+1} - \mathbf{u}_h^{n+1}) \\
& \quad (\|\mathbf{u}_h^{n+1}\|^2 - \|\mathbf{u}_h^n\|^2 + \|2\mathbf{u}_h^{n+1} - \mathbf{u}_h^n\|^2 - \|2\mathbf{u}_h^n - \mathbf{u}_h^{n-1}\|^2 + \|\mathbf{u}_h^{n+1} - 2\mathbf{u}_h^n + \mathbf{u}_h^{n-1}\|^2) \\
& \quad + 4\nu\Delta t\|\nabla \tilde{\mathbf{u}}_h^{n+1}\|^2 - 4s\Delta tb(2\mathbf{B}_h^n - \mathbf{B}_h^{n-1}, \tilde{\mathbf{B}}_h^{n+1}, \tilde{\mathbf{u}}_h^{n+1}) \leq 4\Delta t \left(\frac{\nu^{-1}}{2} \|\mathbf{f}^{n+1}\|_{-1}^2 + \frac{\nu}{2} \|\nabla \tilde{\mathbf{u}}_h^{n+1}\|_{L^2}^2 \right),
\end{aligned}$$

and

$$\begin{aligned}
& 3(\|\tilde{\mathbf{B}}_h^{n+1}\|^2 - \|\mathbf{B}_h^{n+1}\|^2 + \|\tilde{\mathbf{B}}_h^{n+1} - \mathbf{B}_h^{n+1}\|^2) + 2(3\mathbf{B}_h^{n+1} - 4\mathbf{B}_h^n + \mathbf{B}_h^{n-1}, \tilde{\mathbf{B}}_h^{n+1} - \mathbf{B}_h^{n+1}) \\
& \quad (\|\mathbf{B}_h^{n+1}\|^2 - \|\mathbf{B}_h^n\|^2 + \|2\mathbf{B}_h^{n+1} - \mathbf{B}_h^n\|^2 - \|2\mathbf{B}_h^n - \mathbf{B}_h^{n-1}\|^2 + \|\mathbf{B}_h^{n+1} - 2\mathbf{B}_h^n + \mathbf{B}_h^{n-1}\|^2) \\
& \quad + 4\nu_m\Delta t\|\nabla \tilde{\mathbf{B}}_h^{n+1}\|^2 - 4\Delta tb(2\mathbf{B}_h^n - \mathbf{B}_h^{n-1}, \tilde{\mathbf{u}}_h^{n+1}, \tilde{\mathbf{B}}_h^{n+1}) \leq 4\Delta t \left(\frac{\nu_m^{-1}}{2} \|\nabla \times \mathbf{g}^{n+1}\|_{-1}^2 + \frac{\nu_m}{2} \|\nabla \tilde{\mathbf{B}}_h^{n+1}\|_{L^2}^2 \right).
\end{aligned}$$

Using Lemma 4.1 and Lemma 4.2, and summing over times steps gives the stability bound. \square

We now present the convergence theorem:

Theorem 4.2. *Let $(\mathbf{u}_h^{n+1}, \tilde{\mathbf{u}}_h^{n+1}, \mathbf{B}_h^{n+1}, \tilde{\mathbf{B}}_h^{n+1}, p_h^{n+1}, \lambda_h^{n+1})$ be solution to Algorithm 4.1. Assume that (\mathbf{X}_h, Q_h, Y_h) is given by (\mathbf{P}_2, P_1, P_2) , and true solution $(\mathbf{u}, \mathbf{B}, p, \lambda)$ to MHD satisfies the regularity assumptions*

$$\begin{aligned}
& \mathbf{u}, \mathbf{u}_t, \mathbf{B}, \mathbf{B}_t \in L^\infty(0, T; \mathbf{H}^{k+1}(\Omega)), \quad \mathbf{u}_{tt}, \mathbf{B}_{tt} \in L^2(0, T; \mathbf{L}^2(\Omega)), \\
& P, \lambda \in L^2(0, T; L^2(\Omega)).
\end{aligned} \tag{4.10}$$

Then errors satisfy the bound:

$$\begin{aligned}
& \|\mathbf{e}_\mathbf{u}^N\|_{L^2}^2 + \|2\mathbf{e}_\mathbf{u}^N - \mathbf{e}_\mathbf{u}^{N-1}\|_{L^2}^2 + s(\|\mathbf{e}_\mathbf{B}^N\|_{L^2}^2 + \|2\mathbf{e}_\mathbf{B}^N - \mathbf{e}_\mathbf{B}^{N-1}\|_{L^2}^2) \\
& + \left(\beta + \frac{2\gamma\Delta t}{3} \right) (\|\nabla \cdot \mathbf{e}_\mathbf{u}^N\|_{L^2}^2 + \|\nabla \cdot (2\mathbf{e}_\mathbf{u}^N - \mathbf{e}_\mathbf{u}^{N-1})\|_{L^2}^2 + s(\|\nabla \cdot \mathbf{e}_\mathbf{B}^N\|_{L^2}^2 + \|\nabla \cdot (2\mathbf{e}_\mathbf{B}^N - \mathbf{e}_\mathbf{B}^{N-1})\|_{L^2}^2)) \\
& + \gamma(\|\nabla \cdot \mathbf{e}_\mathbf{u}\|_{2,0}^2 + s\|\nabla \cdot \mathbf{e}_\mathbf{B}\|_{2,0}^2) + \nu\|\nabla \mathbf{e}_\mathbf{u}\|_{2,0}^2 + s\nu_m\|\nabla \mathbf{e}_\mathbf{B}\|_{2,0}^2 \leq C(h^6 + \Delta t h^3 + h^4 + \Delta t^4),
\end{aligned}$$

where C is a generic constant independent of the time step and mesh size.

4.2 Numerical experiments

This section presents numerical experiments in order to confirm the predicted only if $\Delta t \leq h$ convergence rates of the theory above, and demonstrate the reliability and the effectiveness of the proposed numerical scheme.

4.2.1 Convergence rate verification for 2d test problem

To confirm convergence rates predicted by the theory, analytical solutions are chosen as

$$\mathbf{u} = \langle \cos(y), \sin(x) \rangle^T, \quad \mathbf{B} = (1 + e^t) \langle \sin(y), \cos(x) \rangle^T, \quad P(x + y) := \sin(x + y), \quad \lambda = 0$$

on the unit square $(0, 1)^2$ with the dimensionless parameters $\nu = \nu_m = s = 1.0$, and the stabilization parameters $\gamma = 1.0 = \beta$. The forcing terms \mathbf{f} and $\nabla \times \mathbf{g}$ are calculated from MHD equations. To test the second order convergence rates, both in time and space, we fixed $t^* = 1.0$ and $h = 1.0$. Then, we run Algorithm 4.1 with this data, and we tie h and Δt together via $h = 2\Delta t$. The results of this simulation are given in Table 3, which are consistent with the theoretical results.

Table 3: Velocity and magnetic errors and rates.

h	Δt	$\ \nabla(\mathbf{u} - \tilde{\mathbf{u}}_h)\ _{2,0}$	Rate	$\ \nabla(\mathbf{B} - \tilde{\mathbf{B}}_h)\ _{2,0}$	Rate
1/2	1/4	8.9138e-3	-	2.5728e-2	-
1/4	1/8	2.3041e-3	1.95	6.4753e-3	1.99
1/8	1/16	5.7460e-4	1.99	1.6179e-3	2.00
1/16	1/32	1.4410e-4	2.00	4.0404e-4	2.00
1/32	1/64	3.6177e-5	1.99	1.0093e-4	2.00

4.2.2 Error comparison for a test problem with smaller ν and larger pressure

This numerical experiment focuses on the pressure robustness of the proposed algorithm. One important advantage of grad-div stabilization is that the stabilization parameter γ with the appropriate selection reduces the negative impact of the continuous pressure on the velocity error. To test that, a similar test problem and set up for the 2d-convergence rate test are used, but fixing end time and time step to $T = 1.0$, $\Delta t = 0.01$, taking the dimensionless kinematic viscosity ν , the magnetic resistivity ν_m and true pressure solution as

$$\nu = \nu_m = 0.01, \quad p(x, y) = 1000 \sin(x + 2y).$$

Then, Algorithm 4.1 is run for the stabilization parameters $\gamma = 1.0$ with $\beta = 0.0$, $\beta = 0.2$ and $\beta = 1.0$ on the successively refined meshes. Errors found using Algorithm 4.1 are compared with those found using the non-stabilized method and the standard grad-div stabilization, see Table 4-Table 7. The results reveal that both velocity and magnetic errors of the proposed stabilization are much better with grad-div and modular grad-div even outperforms usual grad-div.

Table 4: Velocity errors and divergences for non-stabilized, standard grad-div and modular grad-div methods with $\gamma = 1.0$, and $\beta = 0.0$.

h	$\ \nabla(\mathbf{u} - \mathbf{u}_h)\ _{2,0}$			$\ \nabla \cdot \mathbf{u}_h\ _{L^2}$		
	No-stab.	Standard	Modular	No-stab.	Standard	Modular
1/2	70.1858	9.2639	4.3063	64.4802	4.7168	2.0078
1/4	56.1433	5.8339	3.2088	54.3847	2.2815	6.2815e-1
1/8	19.2972	2.0683	1.2302	20.5811	3.7320e-1	1.0682e-1
1/16	3.8795	4.5690e-1	2.8433e-1	4.0239	5.0601e-2	1.3906e-2
1/32	5.5027e-1	7.4750e-2	4.6250e-2	5.5921e-1	6.1943e-3	1.2506e-3
1/64	7.1033e-2	1.0492e-2	6.2951e-3	7.1541e-2	7.4677e-4	8.9371e-5

4.2.3 Error comparison on a fixed mesh with varying ν and ν_m

We next compare the velocity, the magnetic field errors of non-stabilized, standard grad-div (with stabilization parameter $\gamma = 1.0$) and modular grad-div methods (stabilization parameters $\gamma = 1.0, \beta = 0.0$) with varying ν, ν_m . We use the same velocity, pressure and magnetic field solutions and set-up as for 2d convergence rate verification. We fix end time and mesh size to $h = \Delta t = 1/32$. The computed errors from these methods are presented in Table 8. Again we observe similar error behaviour in modular and usual grad-div stabilization.

Table 5: Magnetic errors and divergences for non-stabilized, standard grad-div and modular grad-div methods with $\gamma = 1.0$, and $\beta = 0.0$.

h	$ \nabla(\mathbf{B} - \mathbf{B}_h) _{2,0}$			$ \nabla \cdot \mathbf{B}_h _{L^2}$		
	No-stab.	Standard	Modular	No-stab.	Standard	Modular
1/2	60.1579	3.6724	1.4237	74.0051	1.1343	4.2052
1/4	52.5242	2.039	1.0475	43.2434	3.4875	1.5244
1/8	11.142	5.4573	3.4056	7.8045	5.0659e-2	2.3116e-2
1/16	9.6179e-1	7.1980e-2	5.5424e-2	7.9978e-1	3.6215e-3	1.7146e-3
1/32	5.4253e-2	5.2642e-3	4.6204e-3	4.6581e-2	1.7428e-4	5.9038e-5
1/64	2.7386e-3	3.5648e-4	3.3845e-4	2.3390e-3	7.7457e-6	1.3917e-6

Table 6: Velocity/magnetic errors and the divergences for the standard grad-div and modular grad-div methods with $\gamma = 1.0$, $\beta = 0.2$.

h	$ \nabla(\mathbf{u} - \mathbf{u}_h) _{2,0}$		$ \nabla \cdot \mathbf{u}_h $		$ \nabla(\mathbf{B} - \mathbf{B}_h) _{2,0}$		$ \nabla \cdot \mathbf{B}_h $	
	Standard	Modular	Standard	Modular	Standard	Modular	Standard	Modular
1/2	7.9548	3.9568	4.6099	1.9877	2.7646	1.2753	1.0730	4.0730e-1
1/4	5.2648	3.0085	2.2529	6.2227	1.7796	9.6536e-1	3.4152e-1	1.4851e-1
1/8	1.9397	1.1589	3.6799	1.0590e-1	5.0023e-1	3.2431e-1	4.8820e-2	2.2451e-2
1/16	4.4135e-1	2.7008e-1	4.9938e-2	1.3706e-2	6.9303e-2	5.4188e-2	3.4817e-3	1.6583e-3
1/32	7.3531e-2	4.4072e-2	6.1305e-3	1.2312e-3	5.1760e-3	4.5856e-3	1.6528e-4	5.6494e-5
1/64	1.0410e-2	6.0012e-3	7.4127e-4	8.8708e-5	3.5393e-4	3.3798e-4	7.2813e-6	1.3138e-6

Table 7: Velocity/magnetic errors and the divergences for the standard grad-div and modular grad-div methods with $\gamma = 1.0$, $\beta = 1.0$.

h	$ \nabla(\mathbf{u} - \mathbf{u}_h) _{2,0}$		$ \nabla \cdot \mathbf{u}_h $		$ \nabla(\mathbf{B} - \mathbf{B}_h) _{2,0}$		$ \nabla \cdot \mathbf{B}_h $	
	Standard	Modular	Standard	Modular	Standard	Modular	Standard	Modular
1/2	4.1598	2.6385	3.0801	1.6542	0.7345	7.2052e-1	4.1251e-1	2.5612
1/4	3.3140	2.1956	1.4915	5.1554	9.1221	6.5145e-1	1.7923e-1	1.0712
1/8	1.4285	8.6788e-1	2.6121e-1	9.4149e-2	3.2938	2.6296e-1	3.1821e-2	1.7319e-2
1/16	3.7958e-1	2.1264e-1	3.6521e-2	1.2387e-2	5.7988	4.9245e-2	2.6974e-3	1.3543e-3
1/32	6.8827e-2	3.5542e-2	4.3632e-3	1.1090e-3	4.8471	4.4460e-3	1.2592e-4	4.5424e-5
1/64	1.0109e-2	4.8615e-3	5.0538e-4	7.9243e-5	3.4467	3.3590e-4	5.4069e-6	1.0192e-6

Table 8: Velocity and magnetic errors of the non-stabilized, the standard grad-div and modular grad-div methods with varying ν, ν_m .

$\nu = \nu_m$	$ \nabla(\mathbf{u} - \mathbf{u}_h) _{2,0}$			$ \nabla(\mathbf{B} - \mathbf{B}_h) _{2,0}$		
	No-stab.	Standard	Modular	No-stab.	Standard	Modular
1	5.5354e-3	2.8719e-3	3.3856e-4	1.0584e-4	1.0565e-4	1.0563e-4
1e-1	5.5333e-2	9.7612e-3	3.3405e-3	7.3583e-4	2.8420e-4	2.7886e-4
1e-2	5.4413e-1	7.3920e-2	3.0700e-2	5.4526e-2	5.3253e-3	4.7003e-3
1e-3	4.5381	4.2709e-1	1.8163e-1	6.5683	9.5566e-2	6.6716e-2
1e-4	153.84	1.0358	4.2351e-1	154.69	3.2107e-1	1.5732e-1
1e-5	511.46	1.2435	4.9890e-1	516.06	4.347e-1	1.8728e-1
1e-6	543.82	1.2697	5.0820e-1	546.58	4.5134e-1	1.9143e-1

4.2.4 2d Channel flow over a step

This numerical experiment focuses on two dimensional channel flow over a forward/backward step, in the presence of a magnetic field. The domain considered here is a $[0, 30] \times [0, 10]$ rectangle with a 1×1 step five units into the channel at the bottom. The flow with $\nu = 0.001, \nu_m = 1.0$ passes through the channel from left to right. For the velocity, we enforce no slip boundary conditions on the top, bottom and at the step while $\mathbf{u} = \langle \frac{y(10-y)}{25}, 0 \rangle^T$ at the inflow and outflow. For the magnetic field, we enforce $\mathbf{B} = \langle 0, 1 \rangle^T$ on the walls and step. The initial velocity and initial magnetic fields are $\mathbf{u}_0 = \langle \frac{y(10-y)}{25}, 0 \rangle^T$ and $\mathbf{B}_0 = \mathbf{0}$. The correct physical behaviour of the flow is a smooth velocity field that has eddies form and shed behind the step.

The aim in this numerical experiment is to test and compare the proposed scheme with the unstabilized method and standard grad-div stabilization method, and expectation is to catch the true physical behaviour

of the flow with the model and associated discretization on much coarser discretizations than are needed by a direct numerical simulations (DNS).

We here emphasize that the system (4.1) is no longer physical for this numerical experiment because the use of the Laplace term in the Maxwell equation requires the convex domain. However, numerical simulations of this system with the proposed method over forward/backward step still deserves a consideration since they give similar (but not the same) results as the system presented in the next section.

For DNS, We first run the proposed method, Algorithm 4.1, but without the modular grad-div step, with the $(\mathbf{P}_2, P_1, \mathbf{P}_2, P_1)$ fes for to approximate $(\mathbf{u}, p, \mathbf{B}, \lambda)$ on a mesh that provided 568,535 dof (degrees of freedom). We compute to an end-time at $T = 40$ taking $dt = 0.025$, and $s = 0.01$. A resolved MHD solution at $T = 40$ is given in Figure 5. Next the proposed scheme is tested and compared with unstabilized method, and standard grad-div stabilization using the same flow parameters on a coarser mesh that provide 11,458 dof. The stabilization parameters for the modular grad-div are taken as $\gamma = 1.0$, and $\beta = 0.0$, and for the standard stabilization is $\gamma = 1.0$. All computations are run to $T = 40$ by taking time step $\Delta t = 0.02$. The results from these computations are presented in Figure 6. Here the plots reveals that proposed stabilization method gives a much more accurate solution when compared to unstabilized method, and nearly identical to that found using standard grad-div stabilization.

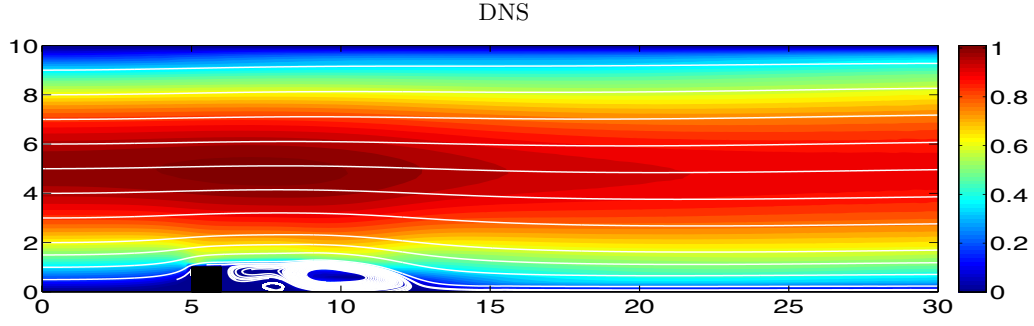


Figure 5: Shown above is the resolved MHD solutions at $T = 40$.

4.2.5 Curl form of the Maxwell Equation

Here, we first present the incompressible MHD flows for which the evolution equations are given by:

$$\begin{aligned} \mathbf{u}_t - \nu \Delta \mathbf{u} + (\mathbf{u} \cdot \nabla) \mathbf{u} - s(\mathbf{B} \cdot \nabla) \mathbf{B} + \nabla P &= \mathbf{f}, \\ \nabla \cdot \mathbf{u} &= 0, \\ \mathbf{B}_t - \nu_m \nabla \times (\nabla \times \mathbf{B}) + (\mathbf{u} \cdot \nabla) \mathbf{B} - (\mathbf{B} \cdot \nabla) \mathbf{u} - \nabla \lambda &= \nabla \times \mathbf{g}, \\ \nabla \cdot \mathbf{B} &= 0, \end{aligned}$$

We emphasize here that the modular grad-div stabilization with the proposed discretization can be applied as in Algorithm 4.1. We

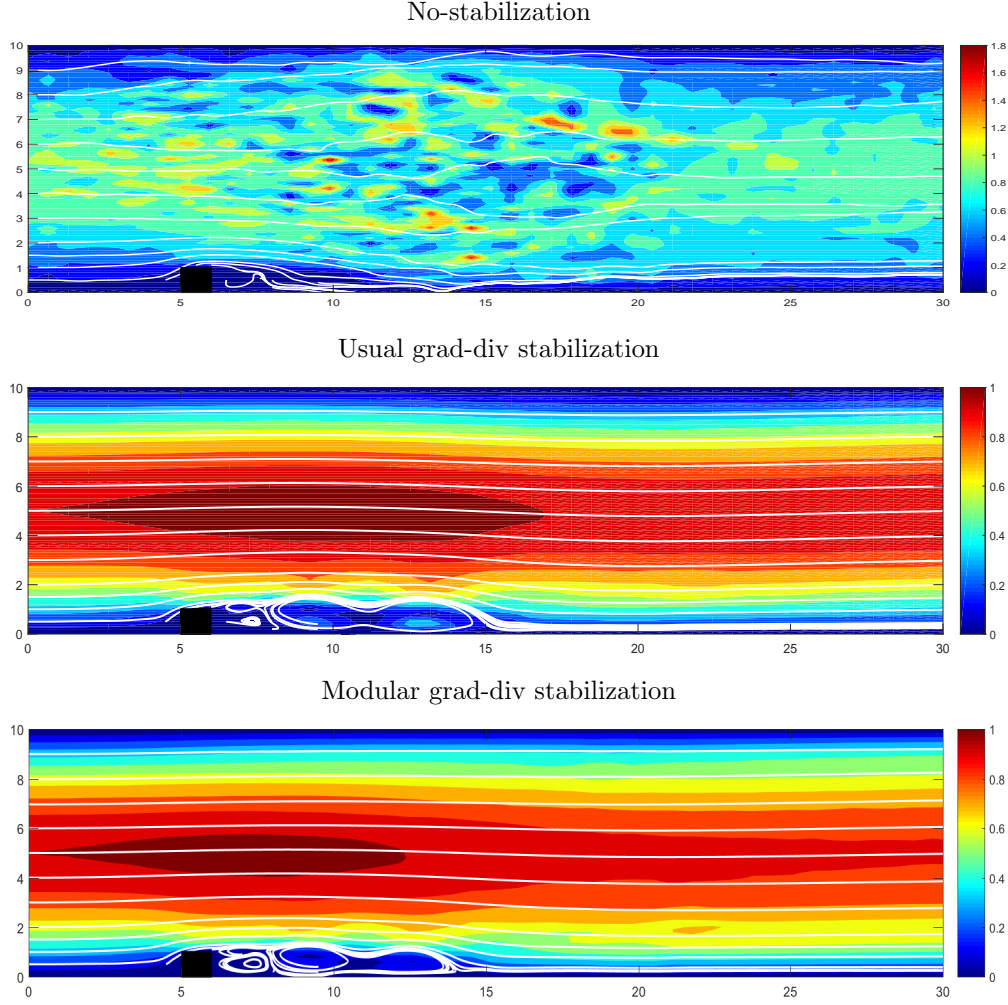


Figure 6: $T = 40$, $\Delta t = 0.02$, $\gamma = 1.0$, $\beta = 0.0$.

5 Conclusions

This paper proposed, analyzed, and tested modular grad-div stabilization methods in discretization of the MHD equations and Boussinesq flows. Unconditional stability and convergence results are established for each flow systems. Numerical experiments were given that verified the convergence rates derived from finite element error analysis. Also, the reliability and efficiency of the methods were tested with some numerical experiments. These results reveal that the methods are very accurate when compared to the non-stabilized methods, and have effects on solutions similar to that of standard grad-div stabilization.

References

- [1] L. Barleon, V. Casal, and L. Lenhart. MHD flow in liquid-metal-cooled blankets. *Fusion Engineering and Design*, 14:401–412, 1991.
- [2] J.D. Barrow, R. Maartens, and C. G. Tsagas. Cosmology with inhomogeneous magnetic fields. *Phys. Rep.*, 449:131–171, 2007.

- [3] D. Biskamp. *Magnetohydrodynamic Turbulence*. Cambridge University Press, Cambridge, 2003.
- [4] P. Bodenheimer, G. P. Laughlin, M. Rozyczka, and H. W. Yorke. Numerical methods in astrophysics. *Series in Astronomy and Astrophysics, Taylor & Francis, New York*, 2007.
- [5] S. Le Borne and L. Rebholz. Preconditioning sparse grad-div/augmented Lagrangian stabilized saddle point systems. *Computing and Visualization in Science*, 16(6):259–269, 2015.
- [6] S. Brenner and L. R. Scott. *The Mathematical Theory of Finite Element Methods*. Springer-Verlag, 2008.
- [7] C.J. Cotter and J. Thuburn. A finite element exterior calculus framework for the rotating shallow-water equations. *J. Comput. Phys.*, 257 (Part B):1506–1526, 2014.
- [8] P. A. Davidson. An introduction to magnetohydrodynamics. *Cambridge Texts in Applied Mathematics, Cambridge University Press, Cambridge*, 2001.
- [9] E. Dormy and M. Nunez. Introduction [special issue: Magnetohydrodynamics in astrophysics and geophysics]. *Geophys. Astrophys. Fluid Dyn.*, 101:169, 2007.
- [10] E. Dormy and A. M. Soward. Mathematical aspects of natural dynamos. *Fluid Mechanics of Astrophysics and Geophysics, Grenoble Sciences. Universite Joseph Fourier, Grenoble*, VI, 2007.
- [11] O. Dorok, W. Grambow, and L. Tobiska. Aspects of finite element discretizations for solving the Boussinesq approximation of the Navier-Stokes Equations. *Notes on Numerical Fluid Mechanics: Numerical Methods for the Navier-Stokes Equations. Proceedings of the International Workshop held at Heidelberg, October 1993, ed. by F.-K. Hebeker, R. Rannacher and G. Wittum*, pages 50–61, 1994.
- [12] J. A. Fiordilino, W. Layton, and Y. Rong. An efficient and modular grad-div stabilization. *Comput. Methods Appl. Mech. Engrg.*, 335:327–346, 2018.
- [13] J. A. Font. General relativistic hydrodynamics and magnetohydrodynamics: hyperbolic system in relativistic astrophysics, in hyperbolic problems: theory, numerics, applications. *Springer, Berlin*, pages 3–17, 2008.
- [14] P. Frolkovic. Consistent velocity approximation for density driven flow and transport. *Advanced Computational Methods in Engineering, Part 2*, pages 603–611, 1998.
- [15] K. Galvin, A. Linke, L. Rebholz, and N. Wilson. Stabilizing poor mass conservation in incompressible flow problems with large irrotational forcing and application to thermal convection. *Comput. Methods Appl. Mech. Engrg.*, 237–240:166–176, 2012.
- [16] S. Ganesan, G. Matthies, and L. Tobiska. On spurious velocities in incompressible flow problems with interfaces. *Comput. Methods Appl. Mech. Engrg.*, 196(7):1193–1202, 2007.
- [17] J. F. Gerbeau, C. Le Bris, and M. Bercovier. Spurious velocities in the steady flow of an incompressible fluid subjected to external forces. *Internat. J. Numer. Methods Fluids*, 25(6):679–695, 1977.
- [18] P. M. Gresho, R. L. Lee, S. T. Chan, and J. M. Leone Jr. A new finite element method for incompressible or Boussinesq fluids. In *Proceeding of the Third international Conference on Finite Elements in Flow Problems*. Wiley, 1981.
- [19] H. Hashizume. Numerical and experimental research to solve mhd problem in liquid blanket system. *Fusion Engineering and Design*, 81:1431–1438, 2006.
- [20] F. Hecht. New development in freefem++. *J. Numer. Math.*, 20(3-4):251–265, 2012.

- [21] J. Heywood and R. Rannacher. Finite element approximation of the nonstationary Navier-Stokes problem. Part IV: Error analysis for the second order time discretization. *SIAM J. Numer. Anal.*, 27(2):353–384, 1990.
- [22] W. Hillebrandt and F. Kupka. Interdisciplinary aspects of turbulence. *Lecture Notes in Physics, Springer-Verlag, Berlin*, 756, 2009.
- [23] E. Jenkins, V. John, A. Linke, and L. G. Rebholz. On the parameter choice in grad-div stabilization for the Stokes equations. *Adv. Comput. Math.*, 40(2):491–516, 2014.
- [24] V. John and A. Kindl. Numerical studies of finite element variational multiscale methods for turbulent flow simulations. *Comput. Methods Appl. Mech. Engrg.*, 199(13-16):841–852, 2010.
- [25] V. John, A. Linke, C. Merdon, M. Neilan, and L. Rebholz. On the divergence constraint in mixed finite element methods for incompressible flows. *SIAM Rev.*, 59(3):492–544, 2017.
- [26] L. D. Landau and E. M. Lifshitz. *Electrodynamics of Continuous Media*. Pergamon Press, Oxford, 1960.
- [27] W. Layton. *An Introduction to the Numerical Analysis of Viscous Incompressible Flows*. SIAM, Philadelphia, 2008.
- [28] W. Layton, C. Manica, M. Neda, M. A. Olshanskii, and L. Rebholz. On the accuracy of the rotation form in simulations of the Navier-Stokes equations. *Journal of Computational Physics*, 228(9):3433–3447, 2009.
- [29] A. Linke, G. Matthies, and L. Tobiska. Robust arbitrary order mixed finite element methods for the incompressible Stokes Equations with pressure independent velocity errors. *ESAIM:M2AN*, 50(1):289–309, 2016.
- [30] A. Linke and C. Merdon. On velocity errors due to irrotational forces in the Navier-Stokes momentum balance. *J. Comput. Phys.*, 313:654–661, 2016.
- [31] A. Linke and C. Merdon. Pressure robustness and discrete Helmholtz projectors in mixed finite element methods for the incompressible Navier-Stokes equations. *Comput. Methods Appl. Mech. Engrg.*, 311:304–326, 2016.
- [32] A. Linke, L. Rebholz, and N. E. Wilson. On the convergence rate of grad-div stabilized Taylor-Hood to Scott-Vogelius solutions for incompressible flow problems. *J. Math. Anal. Appl.*, 381:612–626, 2011.
- [33] J.-G. Liu, C. Wang, and H. Johnston. A fourth order scheme for incompressible Boussinesq equations. *Journal of Scientific Computing*, 18(2):253–285, 2003.
- [34] X. Lu and Huang P. A Modular grad-div stabilization for the 2D/3D nonstationary incompressible Magnetohydrodynamic equations. *Journal of Scientific Computing*, 2020.
- [35] C. Manica, M. Neda, M. A. Olshanskii, and L. Rebholz. Enabling accuracy of Navier-Stokes-alpha through deconvolution and enhanced stability. *ESAIM: Mathematical Modelling and Numerical Analysis*, 45(2):277–307, 2011.
- [36] M. Olshanskii and A. Reusken. Grad-div stabilization for Stokes equations. *Math. Comp.*, 73(248):1699–1718, 2004.
- [37] M. A. Olshanskii. A low order Galerkin finite element method for the Navier-Stokes equations of steady incompressible flow: a stabilization issue and iterative methods. *Comput. Meth. Appl. Mech. Engrg.*, 191(47-48):5515–5536, 2002.

- [38] M. A. Olshanskii, G. Lube, T. Heister, and J. Löwe. Grad-div stabilization and subgrid pressure models for the incompressible Navier-Stokes equations. *Comput. Methods Appl. Mech. Engrg.*, 198(49-52):3975–3988, 2009.
- [39] A. Fierros Palacios. The Hamilton-type principle in fluid dynamics. *Springer, Vienna. Fundamental and applications to magnetohydrodynamics, thermodynamics, and astrophysics.*, 2006.
- [40] D. Pelletier, A. Frodin, and R. Camarero. Are fem solutions of incompressible flows really incompressible? (or how simple flows can cause headaches!). *Internat. J. Numer. Methods Fluids*, 9(1):99–112, 1989.
- [41] B. Punsly. Black hole gravitohydrodynamics. *Astrophysics and Space Science Library, Springer-Verlag, Berlin, second*, 355, 2008.
- [42] Y. Rong and J. A. Fiordilino. Numerical analysis of a BDF2 modular grad-div stabilization method for the Navier-Stokes equations. *Arxiv Preprints*, 2018.
- [43] S. Smolentsev, R. Moreau, L. Buhler, and C. Mistrangelo. MHD thermofluid issues of liquid-metal blankets: Phenomena and advances. *Fusion Engineering and Design*, 85:1196–1205, 2010.
- [44] J. Thuburn and C.J. Cotter. A framework for mimetic discretization of the rotating shallow-water equations on arbitrary polygonal grids. *SIAM J. Sci. Comput.*, 34(3):B203–B225, 2012.
- [45] L. Tobiska and R. Verfürth. Analysis of a streamline diffusion finite element method for the Stokes and Navier-Stokes equations. *SIAM J. Numer. Anal.*, 33(1):107–127, 1996.